Response to reviewer 1

We thank Prof. Bohrer for the constructive comments and suggestions.

P4L7 - Prognostic models predict the result in a future timestep (relative to the times- tamp of observations they ingest). I think you mean here "diagnostically".

Corrected.

P4L9 – I think you somewhat misrepresent the meaning of prognostic and diagnostic models. The difference between the two is that diagnostic model does not include a time evolution. Neither of your terms requires time evolution. Please remove the terms "prognostic" and "diagnostic". I think the best rems to use here with be "directly" and "indirectly". Also see https://earthscience.stackexchange.com/questions/924/model-types- robust-diagnostic-versus-prognostic for a good explanation.

Thanks for pointing this out. We have removed the terms prognostic and diagnostic. The section now reads like this: "*Under these constraints, a strategy is needed to evaluate the TKE budget. The dominant mechanical production term, the buoyant production/destruction term and the dissipation term will be evaluated directly from the data. The residual of the TKE budget will be described as the imbalance as per equation 3 which would contain the effects of advection and transport terms*."

P4 where did eq. 4 come from (it is not in Banerjee et al 2016)? And how come it does not include the roughness length?

The equation is defined inline in Banerjee et al., 2016 after equation 3. However, two new references are added, where they are defined more explicitly (Li et al., 2016 and Kaimal and Finnigan, 1994). The roughness length comes in the equation for the profile of the mean longitudinal velocity, which can be derived by integrating equation 4. The roughness length comes as the lower integration constant. The gradient of velocity should be independent of the surface boundary condition.

P4L20 I recommend making this a numbered equation (the new eq 5), as this is a key component of your calculation, and you don't want to make the reader fish it out of the inline.

Agreed and changed to numbered equation.

P4L26 Can you show the results of this regression (perhaps in an appendix)? What was its R^2? As you can use a whole range or r values to calculate epsilon, how did you actually do

it? Picked a particular r? using the average with all possible r values (given your observation timestep and wind speed) within the 0.2-2 m range? Please add an equation stating the exact and complete formulation of epsilon the way you actually calculated it.

Since it has been a standard technique, it is not repeated in the main text and just the references are added. It is only discussed in the letter following Salesky 2013.. As mentioned in the text, the scaling relation used is $D_{uu}(r) = C_u \epsilon^{2/3} r^{2/3}$,

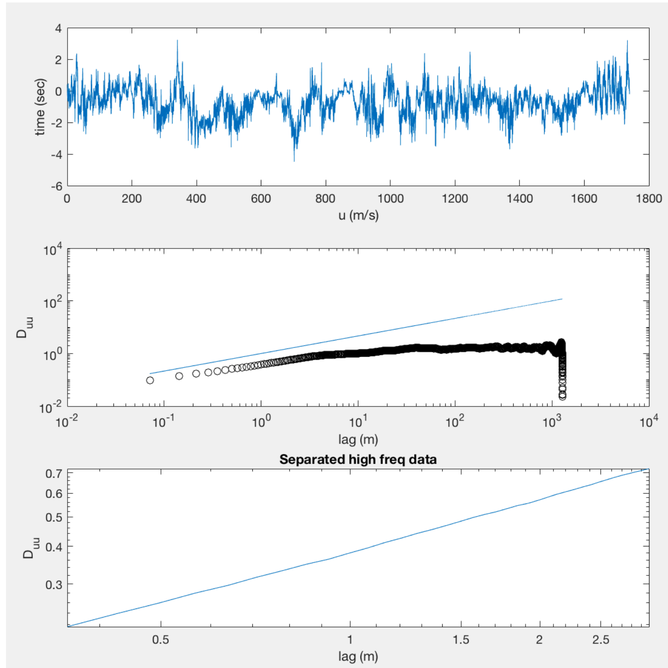

where$c_2 \approx 4.017 c_k$,$c_k = 18 c_e / 55$, and $c_e = 1.5$ is the Kolmogorov constant for the inertial range of the TKE spectrum E(k). Our estimate of ϵ was calculated by a linear regression to the compensated second-order structure function $r_1^{-2/3} D_{11}(r_1)$, i.e., $r_1^{-2/3} D_{11}(r_1) = c_2 \epsilon^{2/3} = a r_1 + b$,

using values of r1 in the range 0.2 ≤ r1 ≤ 2.0 m. The lower limit imposed on r1 ensures that distortions from the sonic anemometer finite path length are negligible. The upper limit on r1 is selected so as to ensure at least one decade of scales is available in the determination of ε. The regression coefficient b was used to obtain an estimate of the dissipation rate (i.e., $\varepsilon = (b/c_2)^{3/2}$); the coefficient a must be nearly zero if the data follow inertial-range scaling. The top panel of the attached figure shows a sample half hour high frequency time series. The middle panel shows the 2/3 scaling fit to the structure function and the third panel shows the extracted dataset between the r range 0.2-2.

Figure 2 – I assume you mean the half-hourly means (or is it the hourly? Daily?) Please state it in the caption.

Half hourly, mentioned in caption now.

P7L6 (and in the description of all other figures) in "thicker" and "thinner" lines, I assume you mean "black" and "red" lines?

Yes, corrected. Thanks for pointing this out. We also corrected the same mistake on P9L5. These two instances remained after we changed the thick - thin scheme which was used in the earlier version of the manuscript.

P7L3-6 this entire section (and similar sections that follow each of your figures) be- longs in the figure caption and not in the text. You should move this to the captions of figs 2 and 3, and start section 3.1 stating: "Our observations show that the desert in associated with higher wind speed . . .(Fig. 2). . .". I have the exact same problem with the first few line of section 3.2. Also, P10L7-11 should be removed (it is already in the caption). These are just examples, the same problem exist in many in other places.

We have faced instances where reviewers had felt uncomfortable without figure descriptions in the main text body although they were in the caption - since this is a subjective editorial issue, we are not changing this style at this time.

P7L9 I totally do not agree that the increase of u_* over the desert after 24th August "can be attributed to mesoscale motions appearing over the region". I think that this is a very simple and direct result of the change in tower height. I do not accept your claim (P6L11-12) that "However, the raising of the mast should not have affected the measurement of turbulent fluxes since it was done within the constant flux layer" - Obviously, and as clearly expressed in your observations - it did.

Accepted. Changed to "*This can be attributed to the raising of the tower height*". Also deleted the sentence : *"However, the raising of the mast should not have affected the measurement of turbulent fluxes since it was done within the constant flux layer"*.

P8L6 "however, after 24th August, the levels of w'w'. . ." Similarly, it is rather easy to claim that it is due to changing the tower height. As the vertical profiles of w'w' are different between the desert and forest (due to roughness length differences), the observed differences between w'w' are a function of observation height. Apparently at 15 m above the desert and 19 m above the forest are high enough to be at the "constant flux layer", the vertical profiles of TKE (u'u' + w'w') converge. However, when you observed at lower elevation, and apparently below the constant flux layer, your data show clear differences in w'w'. As currently stated, without explicitly reminding the reader about the elevation change at that exact date, this statement is highly misleading, especially as it is immediately followed by "Thus. . ." (next sentence, L7).

Accepted. The sentences describing the effect of large scale structures for $\overline{u'u'}$ *and* $\overline{u'w'}$ *are removed as well*. The section is replaced by:

The vertical velocity variance $\overline{w'w'}$ *over the forest is higher than its desert counterpart, however, after 24th August, the levels of* $\overline{w'w'}$ *over desert increases as well and become similar to the forest. It is due to changing the tower height. As the vertical profiles of* $\overline{w'w'}$ *are different between the desert and forest (due to roughness length differences), the observed differences* *between $\overline{w'w'}$ are a function of observation height. At 15 m above the desert and 19 m above the forest are high enough to be at the "constant flux layer", the vertical profiles of TKE ($\overline{u'u'}$+$\overline{w'w'}$) converge. However, when observed at a lower elevation, and below the constant flux layer, the data show clear differences in $\overline{w'w'}$.*

Further in the same point: P9L14 "Although the effect of the large scale structure after 24th August seems to dampen the [dissipation] over the desert while its effects on the [dissipation] over the forest are not very conspicuous." Here, again, it is rather clear to me that you record less TKE dissipation when you are further from the ground and above the roughness sub-layer. One strong argument for observed changes after Aug 24 being tower-height effects rather than change of forcing is that you only observe changes in the desert after the 24th, while the forest observation keep a rather consistent dynamics. You only changed the height of the desert tower, however, a change of forcing should be apparent over both forest and desert.

Agreed. This section is rewritten as : "*A smaller TKE dissipation is recorded when the measurement location is further from the ground and above the roughness sub-layer. One strong argument for observed changes after Aug 24 being tower-height effects rather than change of any large scale forcing is that changes in the desert are observed only after the 24th, while the forest observations maintain a rather consistent dynamics.*"

Fig 4 – what is "full TKE production"? You did not define such term, and if it is the e from eq 1, your data does not allow calculating it. I guess it is the sum of the mechanical and shear production terms. Please state it explicitly and do not call it "full TKE".

It is defined as the summation of mechanical and buoyant TKE production.

ALL figures - Please list in the caption the exact same symbols you used on the figures' y axes, so it is easier to understand what they are, and which is which. Currently you either ignore the symbols (e.g. fig 4), or provide a different version of the symbols on the caption than what is listed on the axes (e.g. fig 7 top 3 panels).

Please note that all terms are listed on the section of the text describing the figure. This way, the caption and the figure description are not exactly the same, referring to Your earlier point.

P9L7 remove "also". You already say "and"

Removed.

P9L12 "huge" is a very subjective term. Perhaps "significant" (if you tested it) or "large" or simply "a" difference (can you calculate and state the % difference?)

Agreed and removed huge. The % difference changes with time, following the exact same trend as the actual terms. replaced by: "*It also indicates that mechanical forcing, and not buoyancy makes a difference (mechanical production is higher by approximately an order of magnitude than buoyant production) in the turbulence generation over the desert and the forest*".

Fig 5 – Explain what are the blue lines, and in the caption or on the figures (as in fig 6) provide the regression statistics (R^2, significance P) for the trend lines (blue?) that you are plotting.

This figure is now removed as we realized that it is not conveying much more information other than what is already there in figure 6.

Fig 6 Provide also the significance P.

p : 0.05.

P13L4 I do not understand why a larger integral eddy time scale over the desert is an indicator of "the transport by secondary circulations above the desert." I think it is indicative of buoyant production of turbulence, which generates larger eddies than shear production.

Agreed and corrected.

P14 – Please combine eq 8-10 to a single equation that relates sigma_u/u* to alpha. It is easy to see that eq 10 is totally redundant (you are re-assigning a fixed number) , and neither eq 8 or 9 are too complicated to allow direct substitution (B1 is a simple additive term in eq 8).

This section is now removed. We agree with Your argument.

P14L11 How do you determine that "The data over the desert is found to be ill conditioned to compute alpha"? I think it'll be more accurate to say that this empirical formulation was originally derived for forests (using data from forest flux towers) and therefore, the values of A_1 and C"_k for the desert are unknown.

This section is now removed.

Fig 8 – draw a dashed line for alpha=1 (but, as you can see below, I rather you removed this figure altogether) Section 3.5 – I totally do not understand what you learn from the VLSM analysis (shown in bottom panel fig 8). During the entire section, you explain how to calculate alpha, and provide excuses for not calculating it over the desert, and not being unable to use it to show sea breezes and other obvious large scale circulation patterns. The only actual informative stamen you make about VLSM is that "there are a number of large peaks of ↲ > 1 after 24th August which confirms the presence of VLSM and supports the interpretations of previous findings in this manuscript". I need to point out that there is presence of large peaks also before 8/24. In fact, larger (Aug 15 is the largest peak) and more (especially if you bundle up the adjacent peaks on the morning of Aug 27) peaks are present before you changed the tower height. Later, in the conclusions section (bullet point 4) you state that "The VLSMs are found to enhance turbulence fluxes and the nonlocal motions for both the forest and the desert. Although its main effect is to enhance the secondary circulations already existing over the desert transporting energy towards the forest." How do you reach this conclusion? Did you measure the correlation between alpha and turbulent fluxes? Can you prove that it enhances the mesoscale circulation already existing? This is purely speculative. If the reason for section 3.5 and conclusion point 4 is to provide justification for all the false claims about the effect of changing the tower height – than it doesn't work. It totally doesn't make a strong case to convince me that there was not effect of tower height. However, I do not understand the insistence on this entire point. Your conclusions do not rely in any way on the tower height and all the things you show about imbalance are valid before and after Aug 24, so why get yourself into this problem. Simply point out the places where the tower height may have influenced the observations, and further point out that the imbalance and other observations from which you draw conclusions about mesoscale circulations and TKE advection are showing similar patters regardless of the tower height. I will be happy if you remove this section and the 4th point of the conclusions.

Agreed. We have now removed the section and the 4th point of the calculation. Earlier discussions have now also pointed out the changes after 24th occurs due to tower height change.

Response to Reviewer 2

This manuscript utilizes a combination of high-frequency, eddy covariance measurements coupled with two Doppler wind lidars, conducted during a 12-day summer period over a desert/forest interface, with the aim of assessing the extent of the secondary circulations previously observed at this site. Additionally, the simplified TKE budget is used to explain the discrepancies between the individual budget terms over the desert and the forest. The observed discrepancies are assigned to the presence of mesoscale secondary circulations caused by the marked heterogeneity between the two opposing land use types. The authors analyze time series and scatterplots of relevant quantities (first, second and third order statistical moments), as well as some derived quantities (integral length scales $In_{u,w}$, CBL depth δ, bulk parameter α). The authors conclude that the TKE budget terms (especially the imbalance term Imb) contain signatures of the aforementioned secondary circulations.

The manuscript provides a genuine view of the secondary circulations over a heterogeneity interface, which are currently held responsible for the surface energy balance non-closure. Hence, the study provides an important contribution to the understanding of a long-standing issue in boundary layer meteorology. The methodology implemented by the authors is well founded and the instrumental setup is sufficient for this purpose. However, the current version of the manuscript suffers from a number of critical drawbacks that the authors have not addressed, or have addressed very poorly. The manuscript requires major revisions prior to its acceptance for publication.

We thank the reviewer for the constructive comments and suggestions.

Major comments

page 4, line 10: You should cite some relevant work done on TKE budgeting, in particular pertaining to how turbulent transport terms, advection terms and the pressure correlation terms may contribute individually over the desert vs. over the forest. Be aware of what may influence the imbalance terms on which your study heavily relies (especially since your Imb also inherently contains the errors from the production and dissipation terms, as stated on line 11 on this page)

Not many instances were found in the literature where the nature of turbulent transport were studied across large scale surface roughness heterogeneities, except for Nadeau 2011 and Yue 2015. These references are now added.

page 4, line 16: The fact that you are conducting a field experiment over gently sloping terrain, immediately calls into place the need for more advanced rotation techniques, and the inclusion of the directional shear term $\overline{v'w'}$ into the definition of friction velocity u_* (Rotach et al, 2008; Wilson, 2008);

$u*$ now contains $\overline{v'w'}$ in its calculation.

page 4, line 17: stability parameter ζ should include the displacement height d, so ζ =(z-d)/L;

It was already calculated using the displacement length d, the text is now corrected.

page 4, line 22: Have you tried estimating ϵ using other indirect methods, for instance the inertial dissipation method?

No, the structure function is used as it usually shows a more robust scaling relation compared to the spectral (inertial dissipation) method since it is calculated in the real space. Moreover, the scaling relation (2/3) in the structure function method can be translated into the scaling relation (-5/3) in spectral space - so ultimately there is not much difference between the two.

page 6, line 10: A mobile mast? Does this mean that the mast was moving around during the 12-day period? If it was not, then please omit mobile because it just distracts;

Removed.

page 6, line 11: Are you confident enough that with being just 9 meters above the canopy top you are above the roughness sublayer? There is no mention of the roughness sublayer here, and there should be one - particularly because you are applying the flux-gradient version of Monin-Obukhov similarity theory to estimate an important TKE budget term, which becomes invalid if you are within the roughness sublayer;

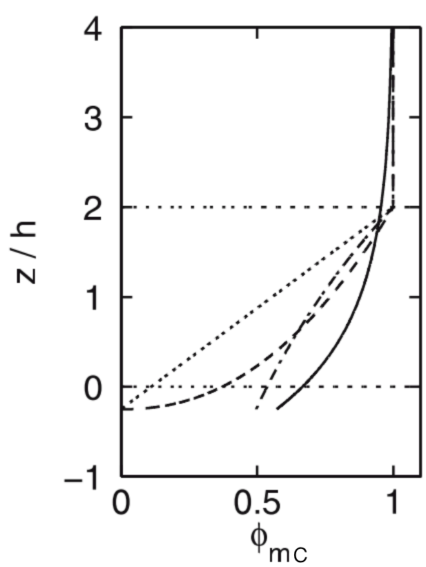

This is a great point and it was already discussed in the first round of revision. As observed from the figure taken from of the roughness sublayer correction function from the paper (figure 2a): Harman, I. N., and J. J. Finnigan, 2007, A simple unified theory for flow in the canopy and roughness sublayer. Boundary-Layer Meteorol., 123, 339–363, its value is about 1 at z/h=2 which is the case in this campaign. This correction function ϕ_{mc} is multiplicative to the original stability correction function ϕ_m. So its value being 1, this is not included. Moreover, it also justifies the fact that we are above the roughness sub layer for both heights 9 m and 18m. We agree that this was not articulated well in the text before. Now it is mentioned.

page 6, line 11: In my opinion, here lies the biggest weakness of this manuscript. First, the raising of the mast occurred on the 23rd, and a lot of subsequent analyses describe the different behavior that suddenly began to occur from the 24th onwards, due to a passage of a large scale mesoscale system. Can you show that there indeed was a large scale system present, for example by showing any before/after upper-level charts? To add to this, you briefly describe the synoptic conditions in the 4th bullet point of the Conclusion (page 16, line 16) - however that information should be moved out of the Conclusion and expanded upon with supporting figures and charts much earlier in the manuscript;

Following the suggestion of reviewer 1, we have removed this sentence. We realized that changing the mast height was indeed responsible for the changes observed after 24th. We have also removed section 3.5 and all discussions of the passage of the large scale structures from the conclusion as well. Changes in individual statistics have been explained in conjunction with the raising of the mast as reviewer 1 suggested. Please see response to reviewer 1.

page 6, line 12: You are simply invoking the constant-flux layer hypothesis with- out citing relevant literature which actually looked at its validity. As it happens, this hypothesis is more often violated than met. Grachev et al (2005), Nadeau et al (2013) and Babic´ et al (2016) are some of the studies that have done this, and found the hypothesis to be true only for certain fluxes and during limited stability conditions. In particular, Babic´ et al (2016) have shown that the sensible heat flux is indeed constant within the daytime surface layer, however this was not true for the momentum flux. Since their study was also conducted over a shrubland, I expect similar to hold in your case (over the desert). My concern is that the raising of the mast by 6 meters may have partially invalidated your conclusions pertaining to the evolution of the friction velocity and consequently mechanical production term after the 24th. Since you don't have at least two lev- els of measurements to estimate the flux divergence, I would highly recommend to cite the relevant literature and insert your view on the potential invalidation of the constant-flux layer hypothesis, especially ways in which your results may be sensitive to assuming that this hypothesis is true.

It is a valid suggestion. To avoid the confusion, we have removed the sentence altogether. As pointed out by reviewer 1, certain changes can indeed be attributed to the change in mast height.

As we have noted later: "*The vertical velocity variance* $\overline{w'w'}$ *over the forest is higher than its desert counterpart, however, after 24th August, the levels of* $\overline{w'w'}$ *over desert increases as well and become similar to the forest. It is due to changing the tower height. As the vertical profiles of* $\overline{w'w'}$ *are different between the desert and forest (due to roughness length differences), the observed differences between* $\overline{w'w'}$ *are a function of observation height. At 15 m above the desert and 19 m above the forest are high enough to be at the "constant flux layer", the vertical profiles of TKE* ($\overline{u'u'}$+$\overline{w'w'}$) *converge. However, when observed at a lower elevation, and below the constant flux layer, the data show clear differences in* $\overline{w'w'}$.

also,

"*A smaller TKE dissipation is recorded when the measurement location is further from the ground and above the roughness sub-layer. One strong argument for observed changes after Aug 24 being tower-height effects rather than change of any large scale forcing is that changes in the desert are observed only after the 24th, while the forest observations maintain a rather consistent dynamics.*"

page 6, line 16: You do not mention how you have pre- and post-processed the eddy covariance data. This also goes for the lidar - you list all these technical specifications (even the serial numbers!), yet you only use the lidar data to calculate the CBL depth. It should be the other way around - the eddy covariance data should be given much larger emphasis in terms of technical specs: What type of sonic anemometers were used? What rotation procedure was applied? How did you detrend the time series? How do you justify the choice of the 30-min averaging time? If all of these are the same as in Fabian Eder's AFM paper, then at least mention this.

We have simply mentioned that the details of the EC method are similar to Eder 2015 paper. More details are added on the rotation technique.

page 7, line 6: But the lower amount of friction over the desert could simply be responsible for higher wind speeds?

Noted and added.

page 7, line 10: On the contrary, this is the perfect opportunity here to discuss the synoptic conditions before and after the 24th. Please include before/after upper-level charts to clearly elucidate the structure of synoptic influence;

Following the argument from reviewer 1**,** This is changed to : "*This can be attributed to the raising of the tower height*".

page 7, line 13: gentle topography and strong vertical updrafts - something that is particularly sensitive to coordinate rotation. Please specify earlier what rotation technique was applied. Wilczak et al (2001) come to mind, who have shown that even a subtle misalignment of the coordinate system may lead to large errors in momentum flux estimates;

Discussion on rotation technique added.

page 10, line 9: Why do you report results for stable stratification all of a sudden? The goal of the manuscript is to try and gain deeper insight into the secondary circulation that causes the DAYTIME energy underclosure, not the NIGHTTIME energy overclosure. Besides, you do not talk about stable conditions hereafter all that much anyway.

We realize that figure 5 is not conveying more information, so it is removed altogether. The same information can be extracted from figure 6.

page 11, line 7: There is a tendency in this paper of very easily assigning the patterns in the Imbalance term to secondary circulations, with oftentimes very far-fetched statements such as this one. Please keep speculations to a minimum when you comment about terms which contain too many variables and uncertain- ties that you can't directly estimate (e.g. the turbulent transport term).

This is a great point and was also raised by reviewer 1 in the previous review. To clarify this issue, we resort to principal component analysis (PCA) which shows the relationships between different variables in a multidimensional data space (not shown in the paper). The first panel shows the centered and scaled data. The second panel shows the total amount of data variability explained by the principal components. As observed, top 2 principal components explain about 80% of the data variability. The 3rd panel shows the 2d biplot and the 4th panel shows the 3d biplot. The angles between the vectors indicate the degree of correlation between the variables. An angle of zero degrees or 180 degrees indicates perfect correlation and orthogonality between the vectors indicate zero correlation.

The biplot confirms that the desert production is highly correlated with the forest production as they should have the same forcing. The desert production is also correlated with the TKE imbalance over the forest. However, the desert production has weaker correlation with desert imbalance. Moreover, the desert imbalance has high correlation with the forest production. The imbalance over desert and forest have almost zero correlation. This indicates that the large scale mostly thermal structures are transported from the desert to the forest. Not all the transport over the desert is generated by the desert production and the large scale nonlocal structures contribute

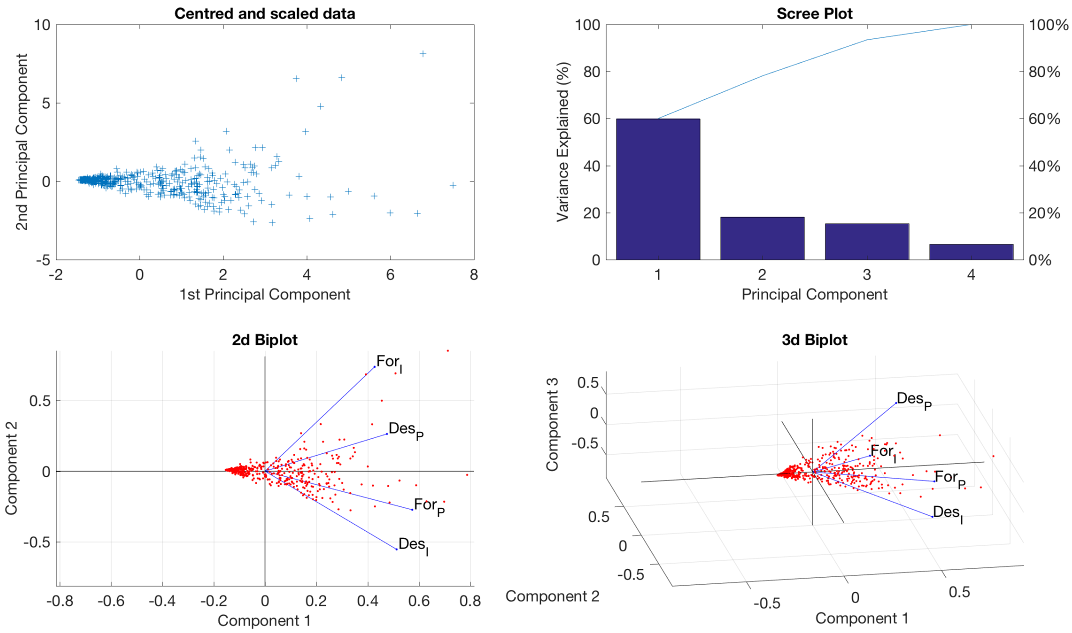

to the transport over the desert, which creates additional forcing over the forest. Thus the high correlation between the desert imbalance and forest production is retained. However, the additional correlations between the desert production and desert imbalance, as well as desert production and forest production are added and acknowledged in the text.

page 11, line 30: Using large scale in conjunction with mesoscale is counterintuitive - did you mean large scale macroscale? If yes, then look at my point earlier above about the need to show upper-level synoptic charts.

As discussed earlier, we have removed all discussions on mesoscale motions.

page 12, line 5: Why suddenly involve sweeps/ejections? The time scale of these coherent structures (hairpin vortices, streaky structures, ramplike convective plumes) is much smaller (20-180 s) than those of secondary circulations (several hours). Besides, secondary circulations do not sweep and eject momentum (in the Theodorsen horseshoe sense) since they are fixed to the heterogeneity interface.

Triple moments have been shown to be connected with sweep-ejection motions (Nakagawa and Nezu, 1977; Raupach et al., 1986; Cava et al., 2006; Katul et al., 2013; Banerjee et al., 2017a). We don't mean to say that the secondary circulations are causing these motions, but the net transport of turbulent energy is causing them.

page 13, line 4: The integral time scale In_u is typically well correlated with the CBL depth . But here you get the opposite: even though the CBL depths over the forest and desert are roughly equal (Fig. 8), the In_u scales show the opposite behavior. Furthermore, I do not see a significant bulk difference in magnitude of the integral scales before and after the 24th, i.e. based on integral scales I would not be confident saying that there was a secondary circulation after the 24th and there was not one before the 24th. I do not see the connection you made with secondary circulations appropriately justifying this discrepancy from a physical standpoint. It looks like you are incorrectly assigning the turnover time of CBL-scale convective thermals (on the order of less than 200 s judging from Fig. 7) to turnover time of secondary circulations (which may last for several hours). If this were true, your autocorrelation function would experience a zero-crossing at much longer time lags (which obviously it does not).

Agreed. This sentence is removed and replaced by what was suggested by reviewer 1: "*More interesting is the observation that the integral time scales for the eddies above the desert are larger than the forest- both of which increase after 24th. This is another indicator of buoyant production of turbulence, which generates larger eddies than shear production*".

page 13, line 8: From Fig. 8, it is obvious that the CBL depths over the forest and desert are almost the same, especially after the 24th. The forest is only slightly larger only on the 18th and the 19th...

This section is now removed.

page 14, line 9: Ill conditioned in what regard?

This section is now removed.

page 14, line 9: Not entirely obvious to me how the forest α would be representative for the desert: When I look at Eq. 8, σ_u (Fig. 3) and δ (Fig. 8) are similar between the forest and desert, but u_* is very different (Fig. 2). This seems to invalidate the justification to extend the forest α to the desert.

This section is now removed.

page 14, line 11: There are only two instances of large α after the 24th, while there are four instances prior to the 24th. Hence this statement is invalid.

This section is now removed.

Figure 8: You don't comment on the apparent tendency for large α (on the 18th, 22nd, 23rd, 24th, 27th) to occur when the CBL is still growing (mostly during morning and early afternoon hours)... Any thoughts on this?

This figure is now removed.

page 14, line 14: This would imply that you would see a low-frequency bump in the vertical velocity spectra, both before and after the 24th. I would like to see a plot of the temporal evolution of the vertical velocity variance profiles from both lidars (perhaps in the form of a time-height Hovmöller diagram?). Maybe something in there would correspond well with the large α instances? I'm aware that Fabian Eder already did something similar in his AFM paper, however he did it only for the 25th-27th period, so after the apparent large scale system passage on the 24th - not before it.

This section is now removed.

Minor comments

page 1, line 16: avoid the use of citations in abstracts.

Removed.

page 3, Equation 1: θ, rather than T , is the traditionally accepted nomenclature for potential temperature(s);

Since we have used T consistently in the paper and other previous papers, it is retained.

page 3, line 25: replace the too-colloquial sheer with large;

Replaced.

page 4, line 7: the word prognostically should come earlier in this subsentence rather than at its end;

As pointed out by reviewer 1, we have removed the terms prognostically and diagnostically.

page 6, line 2: You should emphasize that the Tower 1 location is different from the one analyzed in the cited Eder et al paper.

Mentioned.

page 6, line 11: What are the displacement heights at the forest and the desert sites? See above comment about proper definition of ζ

There is no displacement length considered for the desert. For the forest, it is taken as 2/3rd canopy height.

Figure 1: Please include a map scale and a terrain elevation contour line. As for the north-pointing arrow, please move it to e.g. the top left corner since I barely noticed it in its current position;

Done.

page 6, line 24: So the lidar at tower 2 was working during these outage periods? Why don't you then report its in Fig. 8?

Figure 8 is now removed.

Figure 2 and the following figures: Overbars, rather than brackets, are traditionally used for denoting temporal averages. Brackets are usually used for spatial averaging. There are some inconsistencies: you use brackets around the (co)variances, while in the text you use overbars. Please correct the relevant y- labels. Additionally, specify the x-axis as time in UTC. Finally, I would recommend putting letters to the top corner of each subplot and then accordingly modifying the text to mirror this change.

MATLAB has been used to generate this figures, and a glitch does not allow having over bars in the labels. It has been mentioned that they convey the same thing. time in UTC is mentioned. Letters are not used since there is only one column and each has a specific ylabel.

Figure 3: The momentum flux should have a minus in front of it. Having it with- out one implies that there is a momentum source and mechanical destruction of turbulence (assuming a log law) - which is not in line with the rest of the analyses (where you do indeed have a momentum sink and a corresponding mechanical production of turbulence);

Corrected.

page 7, line 6: The sentence Thicker line indicates desert and thinner line in- dicates forest is a remnant from a prior version of the manuscript before you replaced the thin line with a red line. Remove or modify this sentence.

Corrected.

page 9, line 5: The sentence Thicker line indicates desert and thinner line in- dicates forest is a remnant from a prior version of the manuscript before you replaced the thin line with a red line. Remove or modify this sentence.

Corrected.

page 9, line 8: The start of the sentence Buoyant TKE production over the forest is slightly larger over the forest... is unclear. Please rephrase.

Corrected.

page 10, line 2: Replace on the desert with over the desert.

Done.

page 10, line 4: Replace indicting with indicating.

Corrected.

page 10, line 4: It would be quite instructive to calculate the Pearson correla- tion coefficient between the two Imbalance terms. Also adding a Imb/forest vs. Imb/desert scatterplot to Fig. 6 would be another way of expressing this;

The physical significance of that correlation is not well understood, so we are not adding this. Moreover, from the pca analysis shown before, these two imbalances have almost zero correlation (orthogonal to each other).

Figure 5: I cannot tell the range extent in the stability parameter in some of the subplots... Please make the x-label ticks more numerous.

This figure is now removed.

page 11, line 6: Be careful with wording and speculations here - sounds like you are aiming at studying the turbulent transport term (which naturally you cannot estimate in your case);

Rephrased to : figure 6 is used to better understand the nature of turbulent transport between the desert and the forest.

page 12, Eqs 6 and 7: Is there a reason for not including the ϵ_{uw} and ϵ_{wT} dissipation terms here?

We just wanted to be consistent with the other references provided.

page 12, line 8: ...opposite in nature... sounds ambiguous. Consider rephrasing (for instance ...opposite in sign...).

Corrected.

Figure 8: In the spirit of Figs. 2-7+9, please replace the thin black line with a solid red line.

Figure now removed.

Figure 8: Why interpolate δ on the 21st for the forest, when you don't do it any- where else in the figure?

Figure now removed.

Figure 8: Transform the y-axis into a logarithmic one, given the prevalence of small α.

Figure now removed.

Figure 9: Please consider scaling the averaged vertical velocity on the x-axis with the average Deardorff convective velocity scale w_*;

We wanted to show the strength of the recirculation, so the unit is retained.

Turbulent transport of energy across a forest and a semi-arid shrubland.

Tirtha Banerjee[1,3], Peter Brugger[1], Frederik De Roo[1], Konstantin Kröniger[1], Dan Yakir[2], Eyal Rotenberg[2], and Matthias Mauder[1]

[1]Karlsruhe Institute of Technology (KIT), Institute of Meteorology and Climate Research, Atmospheric Environmental Research (IMK-IFU), 82467 Garmisch-Partenkirchen, Germany

[2]Department of Earth and Planetary Sciences (EPS), The Weizmann Institute of Science, Rehovot 76100, Israel

[3]Current affiliation: Earth and Environmental Sciences Division, Los Alamos National Laboratory, Los Alamos, New Mexico, USA

Correspondence to: Tirtha Banerjee (tirtha.banerjee@lanl.gov)

Abstract. The role of secondary circulations has recently been studied in the context of well defined surface heterogeneity in a semi-arid ecosystem where it was found that energy balance closure over a desert-forest system and the structure of the boundary layer was impacted by advection and flux divergence. As a part of the CliFF (Climate Feedbacks and benefits of semi-arid forests, a collaboration between KIT, Germany and the Weizmann Institute, Israel) campaign, we studied the boundary layer dynamics and turbulent transport of energy corresponding to this effect in the Yatir forest situated in the Negev desert in Israel. The forest surrounded by small shrubs presents a distinct feature of surface heterogeneity, allowing us to study the differences between their interactions with the atmosphere above by conducting measurements with two EC stations and two Doppler LiDARs. As expected, the turbulence intensity and vertical fluxes of momentum and sensible heat are found to be higher above the forest compared to the shrubland. Turbulent statistics indicative of nonlocal motions are also found to differ over the forest and shrubland and also display a strong diurnal cycle. The production of turbulent kinetic energy (TKE) over the forest is strongly mechanical, while buoyancy effects generate most of the TKE over the shrubland. Overall TKE production is much higher above the forest compared to the shrubland. The forest is also found to be more efficient in dissipating TKE. The TKE budget appears to be balanced on average both for the forest and shrubland, although the imbalance of the TKE budget, which contains the role of TKE transport, is found to be quite different in terms of ~~their variation with atmospheric stability and~~ diurnal cycles for the forest and shrubland. The ~~effect of very large mesoscale motions is also directly quantified following a recent formulation by Banerjee and Katul, 2013, using the measured longitudinal velocity variances and boundary layer heights. The~~ difference of turbulent quantities and the relationships between the components of TKE budget are used to infer the characteristics of turbulent transport of energy between the desert and the forest.

1 Introduction

Understanding the interaction between vegetation canopies and atmosphere is a crucial component in quantification of biosphere-atmosphere exchange of heat, carbon dioxide, water and trace gas fluxes. It is also important for the development of numerical weather and climate models where the fluxes in the canopy surface layer (CSL) and the atmospheric surface layer (ASL) are parameterized through bulk exchange coefficients of momentum and scalar. However, idealizations of the forest canopies as horizontally homogeneous momentum sinks and scalar sources introduces uncertainties in flux estimations and estimating diffusion coefficients. Presence of heterogeneities such as roughness transitions, complex topography, mesoscale circulations etc. are common sources of such uncertainties that give rise to nonlocal motions and secondary circulations. These secondary circulations can occur not only in forests but are generic characteristics of boundary layer flows over natural and man made landscapes with discongruity of land use types, surface moisture or temperature etc. (Higgins et al., 2013; Eder et al., 2015). Different types of land covers such as agricultural lands or urban areas can affect local energy balance closure and the structure of the overlying boundary layer as well as cloud formation and regional weather (Eder et al., 2015; Fuentes et al., 2016). Strong difference of surface properties and large swaths of such surface patches are known to induce secondary circulations (Mahfouf et al., 1987; Dalu and Pielke, 1993; Raupach and Finnigan, 1995; Courault et al., 2007; van Heerwaarden and Guerau de Arellano, 2008; Garcia-Carreras et al., 2010; Banerjee et al., 2013; Dixon et al., 2013; Sühring and Raasch, 2013; Kang and Lenschow, 2014; Van Heerwaarden et al., 2014). Recent works by Mauder et al. (2007), Stoy et al. (2013) and Eder et al. (2014) have suggested that non-closure of energy balance is also related to advection and flux divergence due to secondary circulations (Kanda et al., 2004; Foken, 2008). The non-closure of the energy balance refers to the fact that the available energy $R_n - G$ is often higher than the turbulent energy $H + LE$ in micrometeorological sites, where R_n is net radiation, G is soil heat flux, H is sensible heat flux and LE is latent heat flux. Thus it is established that studies involving surface heterogeneities such as difference of roughness characteristics and albedo are crucial for the advancements of our understanding into biosphere-atmosphere interaction since the quasi-universal scaling laws of turbulent moments and simple parametrizations of exchange coefficients are disturbed and rendered non-operational.

Several studies have attempted to study the nature of turbulence across a roughness transition such as a grassland and a forest canopy by means of experimental and numerical methods ~~(Li et al., 1990; Peltola, 1996; Irvine et al., 1997; Belcher et al., 2003; Yang et al~~ documented several length scales associated with the roughness transitions, recirculation zones and as well as the nature of the turbulent momentum budget. However, all of these studies are concerned with the flow adjustment in the immediate vicinity of the roughness transition (edges or gaps). Eder et al. (2015) have studied the dynamics of the convective boundary layer over a well defined surface heterogeneity- namely the Yatir forest and the shrubland surrounding it which are located in the ~~norther~~ northern part of the Negev desert in Israel. Eddy covariance (EC) and Doppler LiDAR measurements were conducted by Eder et al. (2015) in two sites, one in the forest and one in the desert approximately 6.5 km apart. The forest has a darker surface and consequently lower albedo (12.5%) than the desert (33.7 %). Moreover, the higher surface roughness of the forest results in higher turbulence intensity, which leads to more efficient heat transfer above the forest, a phenomenon called canopy convector effect (Rotenberg and Yakir, 2011; Banerjee et al., 2017a). The region being very dry, there is very little latent heat flux (Bowen ratio > 10 over the summer), resulting in spatial difference of surface buoyancy flux of 220-290 Wm^{-2} between the desert and forest. Furthermore, the length scale of surface heterogeneities (6-10 km) is larger than the minimal length scale needed for development of secondary circulations $L_{rau} = C_{Rau} U / w_* \approx 2 - 5$ km (Raupach and Finnigan, 1995; Eder et al., 2015), where U is mean wind speed, w_* is the convective velocity scale and $C_{Rau} = 0.8$, an empirical parameter, so that it is possible for secondary circulations to develop.

The present work is an attempt to examine this hypothesis of secondary circulations in more detail. We use eddy covariance and Doppler LiDAR measurements at two sites over the shrubland and the Yatir forest 4.3 km apart, where the shrubland is upwind of the forest in the path of the principal wind direction (during the summer, there exists a heat induced low pressure system to the east, resulting in the main wind direction from the north west). We investigate the individual components of the turbulent kinetic energy budget, as well as the nature of advection and turbulent transport over the forest and desert and determine if there is a relationship between them. ~~The role of large scale structures is also investigated.~~ Not many instances were found in the literature where the nature of turbulent transport was studied across large scale surface roughness heterogeneities, except for Nadeau et al. (2011) and Yue et al. (2015). However, Yue et al. (2015) only studied turbulent production and the turbulent velocity fluctuations in presence of a complex topography - so the nature of turbulent transport via secondary circulations was not highlighted. Nadeau et al. (2011) studied the decay of turbulence over different land surface types. Hence the difference of turbulence production and simultaneous transport across different land use types were not studied, which determines the scope of the current work.

2 Method

2.1 Theory

The turbulent kinetic energy (TKE) budget without invoking any special assumption is given by (Stull, 2012)

$$\frac{\partial e}{\partial t} + U_j \frac{\partial e}{\partial x_j} = \delta_{i3} \frac{g}{T} \left(\overline{u_i' T'} \right) - \overline{u_i' u_j'} \frac{\partial U_i}{\partial x_j} - \frac{\partial \left(\overline{u_j' e} \right)}{\partial x_j} - \frac{1}{\rho} \frac{\partial \left(\overline{u_i' p'} \right)}{\partial x_i} - \epsilon, \tag{1}$$

where i and j are usual tensor indices which can take the values of 1, 2 and 3, to indicate x, y and z directions respectively and δ_{i3} is the Kronecker delta. $e = (1/2)(\sigma_u^2 + \sigma_v^2 + \sigma_w^2) = (1/2)(\overline{u'^2} + \overline{v'^2} + \overline{w'^2})$ is the TKE, U denotes mean longitudinal velocity, u', v' and w' denote the fluctuations from mean for the longitudinal, transverse and vertical velocity components, g is acceleration due to gravity, T denotes mean potential temperature, T' is the potential temperature fluctuation, p' is the dynamic pressure perturbation, ρ is density of air. The first term on the left hand side (LHS) denotes storage or TKE tendency. The second term on the LHS indicates advection of TKE by mean wind flow. The first term on the right hand side (RHS) denotes buoyant production/destruction of TKE. The second term on the RHS denotes mechanical/shear production of TKE. The third term on RHS denotes turbulent transport of TKE and can also be called turbulent flux divergence. The fourth term on RHS denotes transport of TKE by pressure velocity correlation. ϵ is the dissipation of TKE.

Expanding the equations in terms of x, y and z coordinates, the full TKE budget can be written as equation A1 as shown in appendix A. Since it is difficult to keep track of the full equation due to the ~~sheer~~ large number of terms, it would be easier to use a simple form of the TKE budget (Stull, 2012)

$$0 = -\overline{u'w'} \frac{dU}{dz} + \frac{g}{T} \overline{w'T'} - \epsilon - Imbalance. \tag{2}$$

where the $Imbalance$ is defined in equation A2. Note that $\overline{u'w'}$ and $\overline{w'T'}$ denote vertical momentum flux and sensible heat flux respectively. Also notice that if the term $Imbalance$ is set to zero, one recovers the TKE budget for an idealized surface layer where the coordinate system is aligned with the mean wind, and a planar, homogeneous flow with zero subsidence is assumed. Since our objective in the current problem is to study the effect of heterogeneity, we cannot make these assumptions. Moreover, we are also constrained by being able to measure only at two single points in space quite far apart. Single point eddy covariance measurements cannot compute spatial gradients, and the pressure perturbations are not measured either. Thus explicit computations of the imbalance terms are not possible. Due to the three dimensional nature of the problem, it is also difficult to anticipate what degrees of assumptions are sufficient so that some of the terms can be ignored safely.

Under these constraints, a strategy is needed to evaluate the TKE budget. ~~As will be shown later, we are able to compute the terms in the equation 2 except $Imbalance$ prognostically. Thus the~~ The dominant mechanical production term, the buoyant production/destruction term and the dissipation term will be evaluated directly from the data. The residual of the TKE budget will be described as the imbalance as per equation 3 which would ~~diagnostically~~ contain the effects of advection and transport terms. The advantage of using this strategy is that since the original TKE budget equation has to be closed, the errors in computing the production and dissipation terms can also be assumed to be inside the $Imbalance$ term.

$$Imbalance = -\overline{u'w'}\frac{dU}{dz} + \frac{g}{T}\overline{w'T'} - \epsilon. \tag{3}$$

To compute the mechanical production term, we momentarily assume that the TKE budget is well balanced and Monin Obukhov Stability Theory (MOST) (Monin and Obukhov, 1954) is valid ~~(Banerjee et al., 2016)~~(Kaimal and Finnigan, 1994; Banerjee et al. This allows us to write

$$\frac{dU}{dz} = \phi_m(\zeta)\frac{u_*}{\kappa z}, \tag{4}$$

where ϕ_m is the stability correction function for momentum which varies with the stability parameter $\cancel{\zeta = z/L}$ $\zeta = (z-d)/L$ and $\kappa = 0.4$, the ~~von-Kármán~~ von Kármán constant. $u_* = \sqrt{|\overline{u'w'}|}$ is the friction velocity, z is the measurement height and $L = -u_*^3/(\kappa(g/T)\overline{w'T'})$ is the Obukhov length, d is zero plane displacement height, taken as 2/3 of canopy height. The standard MOST scaling relations for ϕ_m are used, i.e., $\phi_m = 0.74 + 4.7\zeta$ for stable ($\zeta > 0$) and $\phi_m = (1-16\zeta)^{-1/4}$ for unstable ($\zeta < 0$) stratification (Businger et al., 1971; Dyer, 1974).

Equation 4 allows us to compute the mechanical production term in equation 2 as $\cancel{-\overline{u'w'}dU/dz = \phi_m u_*^3/(\kappa z)}$. :

$$-\overline{u'w'}\frac{dU}{dz} = \phi_m \frac{u_*^3}{(\kappa z)}. \tag{5}$$

The buoyancy term can directly be computed from the EC measurements as well. To compute the dissipation term ϵ, we use the scaling relation of second order structure function $D_{uu} = \overline{[u(x+r)-u(x)]^2}$ in the inertial subrange (Salesky et al., 2013; Banerjee et al., 2015, 2016; Li et al., 2016)

$$D_{uu}(r) = C_u \epsilon^{2/3} r^{2/3}, \tag{6}$$

where $C_u \approx 2$ (Stull, 2012), and r is the spatial lag in the longitudinal direction which can be computed by multiplying the sampling time interval with the mean longitudinal velocity, assuming that Taylor's frozen turbulence hypothesis is valid ($r = |u|\,\Delta t$). The range of r where this relation is valid is found to be between 0.2 to 2 m and ϵ is found by regression of equation 6. Note that the computation of ϵ is independent from any assumptions used to compute the production terms.

2.2 Research site

The measurements were conducted in the Yatir forest and the surrounding shrubland in Israel between 18th August and 30th August, 2015 as part of the "Climate feedbacks and benefits of semi-arid forests" (CliFF) campaign, a joint collaboration between Karlsruhe Institute of Technology (KIT), Germany and the Weizmann Institute, Israel. Fig 1 gives an idea about the locations of the EC towers. Tower 1 (Latitude 31.375728, Longitude 35.024262) was located at the semi-arid shrubland 620 m above sea level and tower 2 (Latitude 31.345315, Longitude 35.052224) was located inside the forest 660 m above sea level. The linear distance between the two locations was measured to be 4.3 km and as can be observed from figure 1, there is a distinct surface heterogeneity between the two sites. The climate of the area is in between Mediterranean and semi-arid, with a mean annual precipitation of about 285 mm (Eder et al., 2015). Note that the measurement sites reported in this work are different from those in Eder et al. (2015). The trees in the forest were mostly Aleppo Pine (*Pinus halepensis*), average 10 m in height with negligible height variation. The surrounding land was sparsely populated by small shrubs and in the dry season where the measurements were conducted, was mostly free of vegetation. Thus it is referred to as 'desert' for easy distinction (Eder et al., 2015). The measurement height for the forest was 19 m above ground (9 m above the canopy height). ~~A mobile~~ Note that with this height selection, the measurements were conducted above the roughness sublayer, which ends at approximately 2 times the canopy height (Harman and Finnigan, 2007). A mast was used over the desert and the measurement height was 9 m until 23rd August, after which it was changed to 15 m for the remaining period. ~~However, the raising of the mast should not have affected the measurement of turbulent fluxes since it was done within the constant flux layer.~~ In this zone of the atmospheric surface layer, the longitudinal and crosswise velocity variances decrease logarithmically with height and the vertical velocity variance shows an independence with height (Townsend, 1976; Perry and Chong, 1982; Marusic et al., 2013; Banerjee and Katul, 2013a). ~~Thus there is no evidence to support that increasing of measurement height affected turbulence measurements.~~ High frequency turbulent data were collected at 20 Hz and 30 minutes averaging periods were used for both sites. ~~In addition, two Doppler LiDARs were used at the two locations to measure the boundary layer height as well.~~ After conducting quality control of the data following Eder et al. (2015), a planar fit coordinate rotation is applied on the velocity components since the data is collected on a sloped ground. The coordinate rotation following Wilczak et al. (2001) ensures that the cross stream velocity component v is zero and corrects the tilting of the anemometer with respect to the local streamlines. Moreover, a different set of coordinate rotation is applied for the desert data after 23rd August. More details of the coordinate rotation technique can be found in appendix C.

In addition, two Doppler LiDARs were used at the two locations to measure the boundary layer height as well. The Doppler LiDARs used were StreamLine systems from HaloPhotonics. They were operated in a vertical stare mode most of the time (interrupted every half hour for less than 90 seconds). Technical specifications and instrument settings of the Doppler Li-

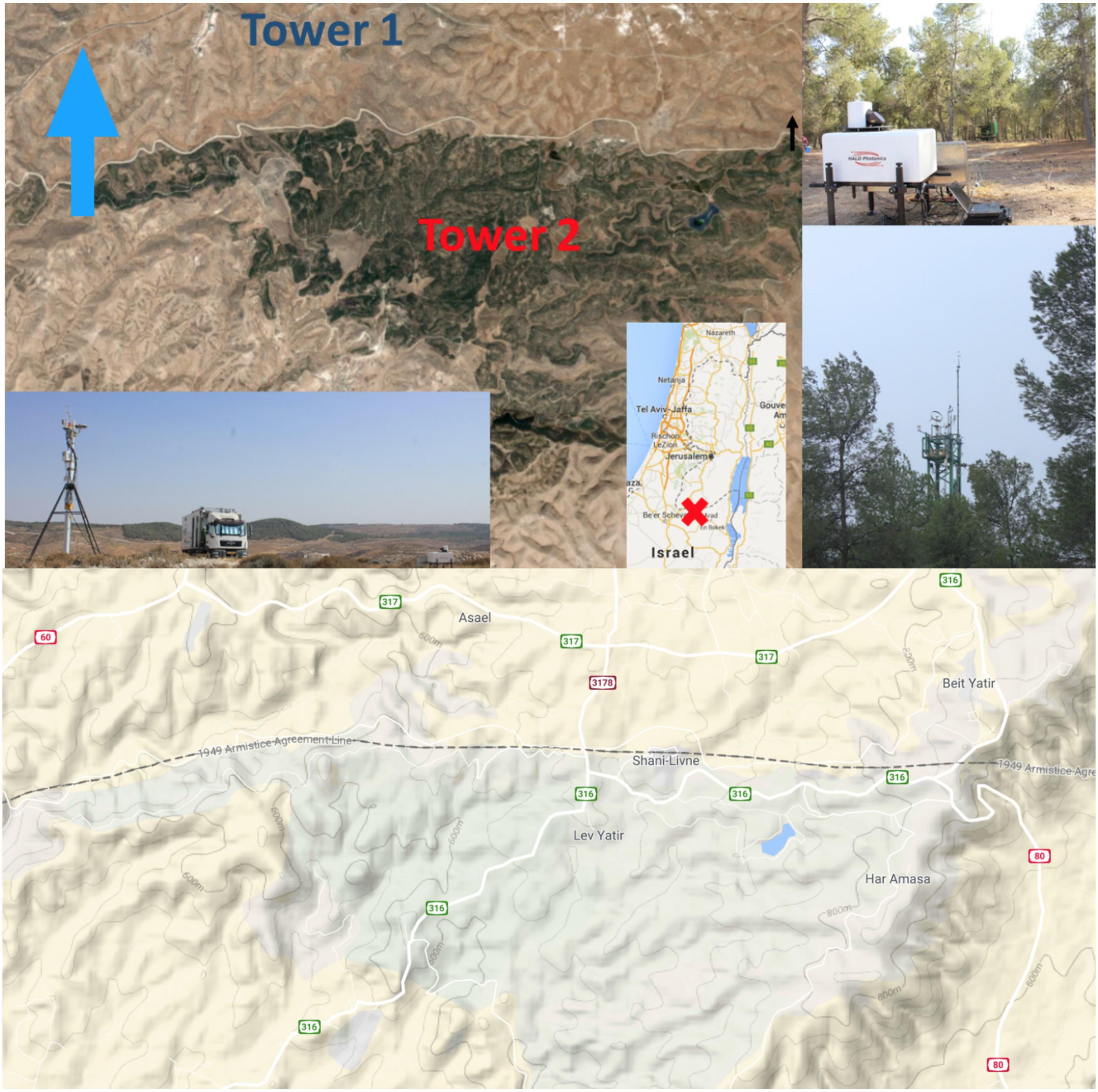

Figure 1. Map of Yatir forest in Israel and locations of the measurement stations. Insets: snapshots of measurement set-ups. Bottom panel: topography map of the Yatir forest, from Google maps.

Table 1. Instrument specification and settings of the Doppler LiDARs. From top to bottom: Serial number of the forest and desert LiDAR, pulse length of the laser pulse at full width at half maximum, range gate length, pulse repetition frequency, number of averaged pulses for a backscatter coefficient profile and the wavelength of the emitted laser pulse (short wavelength infrared).

Serial numbers	0114-74 and 0114-75
Pulse length	60 m
Range gate length	18 m
Pulse repetition frequency	15 kHz
Averaged pulses per estimate	15000
Wavelength of laser light	1.5 μm

DARs are given in Table 1. ~~For retrieval of the boundary layer height the three largest negative backscatter gradients were computed from the backscatter profiles of a 10 minutes interval to estimate aerosol layer heights. Then a modified algorithm of Lotteraner and Piringer (2016) was used for post-processing of the aerosol layer time series to get a time series of the boundary layer height.~~ The Doppler LiDAR at tower 1 was not working from 19.08.2015 - 15:00 UTC until 21.08.2015 - 10:30 UTC and very shortly on the 23.08.2015 around 10:00 UTC due to power cuts.

3 Results and Discussion

3.1 Time series of turbulence statistics

Time series of mean speed ($\mathrm{ms^{-1}}$), mean vertical velocity (W, $\mathrm{ms^{-1}}$) friction velocity (u_*, $\mathrm{ms^{-1}}$), mean near surface air (potential) temperature (T, K), for the measurement period are shown in figure 2. Figure 3 shows time series of longitudinal velocity variance ($\overline{u'u'}$, $\mathrm{m^2s^{-2}}$), vertical velocity variance ($\overline{w'w'}$, $\mathrm{m^2s^{-2}}$), momentum flux ($\overline{u'w'}$, $\mathrm{m^2s^{-2}}$) and sensible heat flux ($\overline{w'T'}$, $\mathrm{Kms^{-1}}$). ~~Thicker~~ Black line indicates desert and ~~thinner~~ red line indicates forest. As noticed, the desert is associated with a higher wind speed ~~and higher mean vertical velocity . Although the~~ because of a lower amount of friction on the desert surface. The higher vertical velocity over the desert indicates the presence of stronger updrafts which would be explained by higher buoyancy driven turbulence. The friction velocity (u_*) over the forest is much higher compared to the desert, especially in the daytime, which is expected because of higher surface roughness over the forest. u_* above both the forest and desert shows a strong diurnal cycle. However, there seems to be a prominent increase of u_* over the desert after ~~24th~~ 23th August. This can be attributed to ~~mesoscale motions appearing over the region, which will be discussed later. The higher mean speeds over the desert indicate of existence of large energetic eddies, possibly associated with secondary circulations. There could be several factors responsible for the secondary circulations. The~~ the raising of the tower height. Moreover, the gentle topography around the desert could result in the strong vertical updrafts above the desert. ~~The consistent presence of the sea breeze from the north west due to the heat induced low pressure system to the west could be another major feature of the secondary circulations. However, the secondary circulations cannot raise the turbulence levels above the desert since mechanical forcing by roughness~~

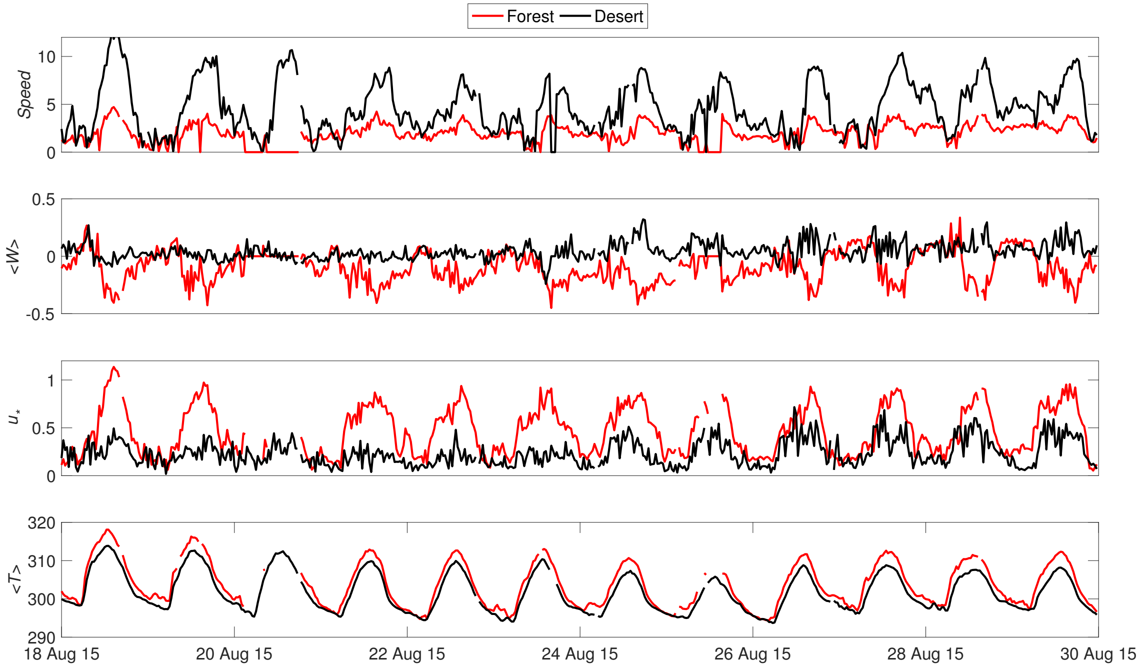

Figure 2. Time series of half hourly averages of mean speed (ms^{-1}), mean vertical velocity (ms^{-1}), friction velocity (ms^{-1}) and mean potential temperature (K) for the measurement period. Black line indicates desert and red line indicates forest.

~~is absent.~~ Interestingly, the near surface air temperatures over both the forest and desert show a strong diurnal cycle ~~but their daytime differences are not very high.~~ and their differences are about 5K on average during daytime and almost zero at night..

The longitudinal velocity variance $\overline{u'u'}$ over the forest and desert show similar variations over time~~, and the effects of a large scale energetic system are also visible in $\overline{u'u'}$ for both the desert and forest~~. The vertical velocity variance $\overline{w'w'}$ over the forest is higher than its desert counterpart, however, after ~~24th~~ 23th August, the levels of $\overline{w'w'}$ over desert increases as well and become similar to the forest. ~~Thus this large scale structure influences the already existing secondary circulation, and it ramps up turbulence levels in both velocity components differently over the desert and the forest~~It is due to changing the tower height. As the vertical profiles of $\overline{w'w'}$ are different between the desert and forest (due to roughness length differences), the observed differences between $\overline{w'w'}$ are a function of observation height. At 15 m above the desert and 19 m above the forest floor are high enough to be at the "constant flux layer", the vertical profiles of TKE ($\overline{u'u'}+\overline{w'w'}$) converge. However, when observed at a lower elevation, and below the constant flux layer, the data show clear differences in $\overline{w'w'}$.

The vertical momentum flux $\overline{u'w'}$ over the forest is much higher compared to the desert-which is also expected because of the higher surface roughness of the forest, making it a much more efficient momentum sink compared to the desert. Note that the shear transport of momentum flux is still much more effective over the forest compared to the desert because of roughness

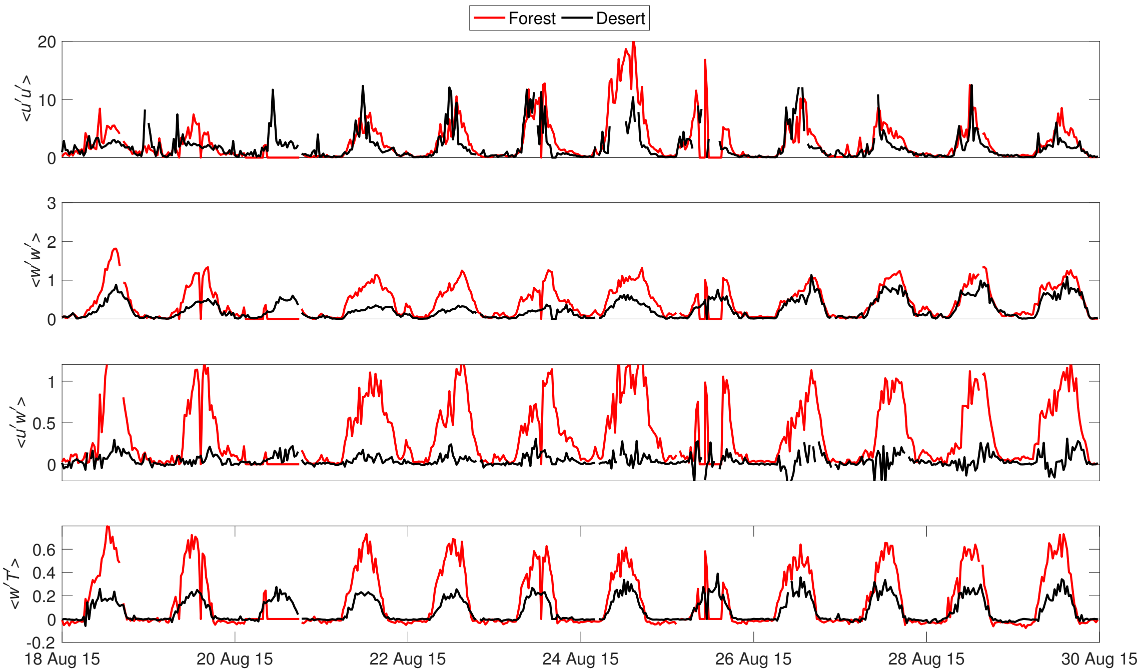

Figure 3. Time series of longitudinal velocity variance ($\mathrm{m^2s^{-2}}$), vertical velocity variance ($\mathrm{m^2s^{-2}}$), momentum flux ($\mathrm{m^2s^{-2}}$) and sensible heat flux ($\mathrm{Kms^{-1}}$) for the measurement period. Black line indicates desert and red line indicates forest.

effects even though the mean quantities can be higher over the desert. The sensible heat flux $\overline{w'T'}$ over the forest is also higher as discussed before due to the canopy convector effect~~, but the mesoscale structure increases the sensible heat flux above the desert after 24th August~~.

3.2 Nature of TKE budget

~~First row: forest, second row: desert. First column: TKE production vs dissipation for stable conditions. Second column: variation of TKE imbalance with stability parameter for stable conditions. Third column: TKE production vs dissipation for unstable conditions. Fourth column: variation of TKE imbalance with stability parameter for unstable conditions.~~

Figure 4 shows the time series of the components of the TKE budget as discussed in section 2.1. The first row shows mechanical production of TKE (P_{Mech}, $\mathrm{m^2s^{-3}}$), the second row shows buoyant production of TKE (P_{Buoy}, $\mathrm{m^2s^{-3}}$), the third row shows full TKE production (P_{TKE}, $\mathrm{m^2s^{-3}}$), ~~the~~ which is the summation of mechanical and buoyant TKE production. The fourth row shows dissipation of TKE (ϵ, $\mathrm{m^2s^{-3}}$) and the fifth row shows imbalance of TKE (Imb, $\mathrm{m^2s^{-3}}$). ~~Thicker~~ Black line indicates desert and ~~thinner~~ red line indicates forest. As noticed in figure 4, the production of turbulence is mostly by mechanical or shear forcing because of the roughness of the forest, whereas mechanical production of TKE over desert is very

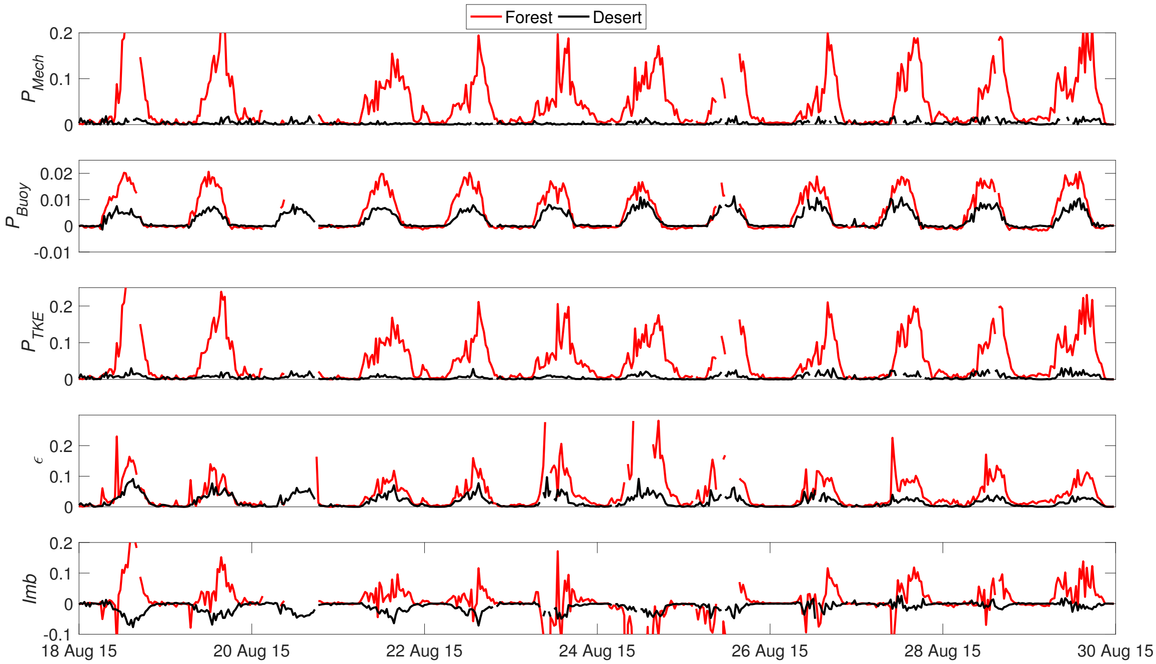

Figure 4. Time series of mechanical production of TKE ($\mathrm{m^2s^{-3}}$), buoyant production of TKE ($\mathrm{m^2s^{-3}}$), full TKE production ($\mathrm{m^2s^{-3}}$), dissipation of TKE ($\mathrm{m^2s^{-3}}$) and imbalance of TKE ($\mathrm{m^2s^{-3}}$). Black line indicates desert and red line indicates forest.

small and does not ~~also~~ have a strong diurnal cycle like the forest, although it increases slightly after ~~24th~~ 23th August. On the other hand, TKE production over the desert is mostly carried by buoyancy. Buoyant TKE production ~~over the forest~~ is slightly larger over the forest~~but of similar order of magnitude as the desert~~. The buoyant TKE production over the desert is also higher after ~~24th~~ 23th August. Given the moderate temperature difference between the desert and the forest, the difference of their corresponding buoyant TKE production is interesting. It also indicates that mechanical forcing, and not buoyancy makes a ~~huge difference~~ difference (mechanical production is higher by approximately an order of magnitude than buoyant production) in the turbulence generation over the desert and the forest. The diurnal cycle of the TKE dissipation ϵ is interesting as well. The dissipation of TKE seems to be higher above the forest as well compared to the desert. ~~Although the effect of the large scale structure after 24th August seems to dampen the ϵ over the desert while its effects on the ϵ over the forest are not very conspicuous.~~

A smaller TKE dissipation is recorded when the measurement location is further from the ground and above the roughness sub-layer. One strong argument for observed changes after Aug 23 being tower-height effects rather than change of any large scale forcing is that changes in the desert are observed only after the 23th, while the forest observations maintain a rather consistent dynamics.

The diurnal cycles of the TKE imbalance computed by equation 3 is also very interesting. The imbalance over the forest is often positive over the daytime, while ~~on~~ over the desert it is often negative, highlighting the difference of turbulent transport and advection over the two different regimes. Also notice that the positive imbalance for forest and negative imbalance for desert almost have a phase (anti)synchronization, indicting that the turbulence above forest and desert are responsive to one another and they are part of a coupled system, indicating again towards the role of the secondary circulations.

~~Figure ?? highlights the nature of TKE budget over the forest and the desert in more details. The first row shows TKE budgets for the forest and the second row shows the same for the desert. The first column shows TKE production vs dissipation for stable conditions. The second column shows variation of TKE imbalance with the stability parameter $\zeta = z/L$ for stable conditions ($\zeta > 0$). The third column shows TKE production vs dissipation for unstable conditions and the fourth column shows the variation of TKE imbalance with stability parameter for unstable conditions ($\zeta < 0$). As observed, the Range of TKE production and dissipation are higher for unstable conditions for both the forest and desert compared to stable conditions. On average, the TKE budget is closed as seen from the one to one solid line for both the desert and forest, although there is more uncertainty in the TKE closure for the desert compared to the forest for both stable and unstable conditions. However, the TKE imbalance for the forest increases with near neutral conditions and reduces as the stratification becomes more convective or highly stable. On the other hand, the TKE imbalance for desert does not change much with stability for the stable conditions and actually increases more with more convective conditions, which is a directly opposite to the nature of TKE imbalance over the forest. This behavior gives us more insight into the nature of turbulent transport over the forest and desert and highlights their difference. More convective conditions means more TKE transport by means of advection, subsidence and flux divergence over the desert.~~

3.3 ~~Transport of TKE over desert and forest~~

~~Figure 5 shows the interrelationship between the nature of turbulent transport over the desert and~~

3.3 Transport of TKE over desert and forest

Figure 5 is used to better understand the nature of turbulent transport between the desert and the forest. Panel (a) depicts the TKE imbalance over desert vs the net production of TKE over the forest. As observed, there is a significant correlation (0.5) between them, indicating that the advection and transport of TKE by flux divergence and pressure fluctuations reach downstream by means of the secondary circulations and produces TKE over the forest. On the other hand, the converse is not true, as observed in panel (b) of figure 5. There is little correlation between the Imbalance of TKE over forest and the production of TKE over desert (0.14). As observed in panel (c), the production over desert is also well correlated with the production over forest (0.3) as both the desert and forest are subjected to the same forcing. However the TKE production over desert is not that well correlated with the TKE imbalance over the desert as seen in panel (d). Thus while there should be some cross correlation in panel (a) because of desert production, that is not the only effect. The nonlocal large scale motions contribute to the transport over desert (without significantly altering TKE production over desert) which in turn cause TKE production above the forest because of the higher mechanical forcing.

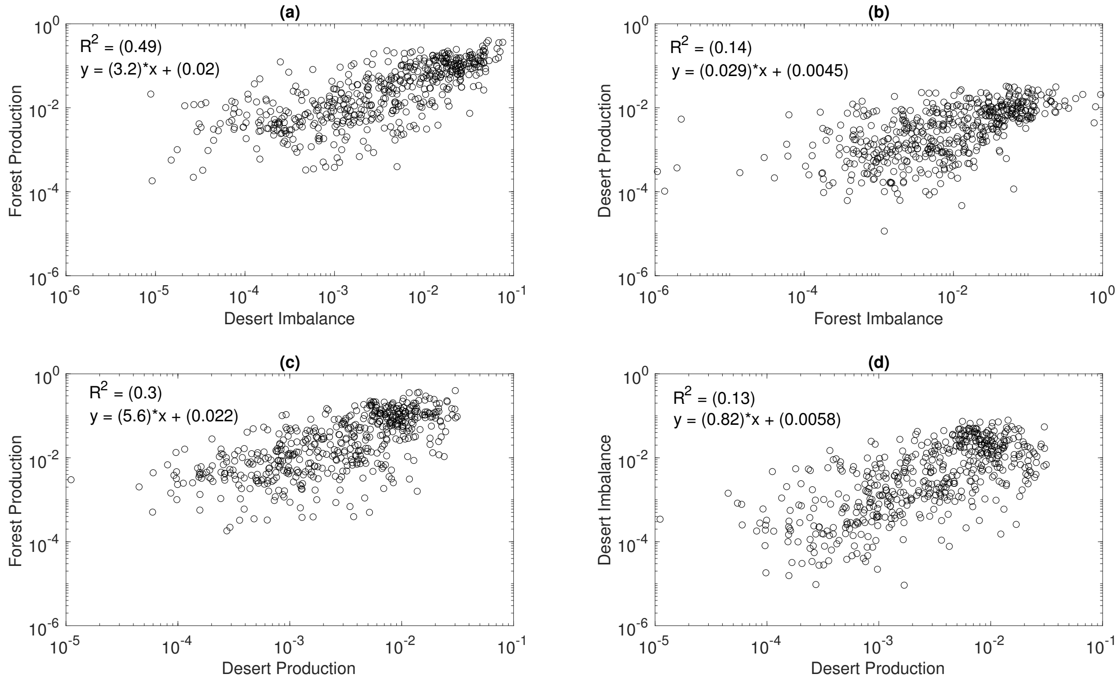

Figure 5. (a) TKE imbalance for desert vs TKE production for forest. (b) TKE imbalance for forest vs TKE production for desert. (c) TKE production for desert vs TKE production for forest. (d) TKE production for desert vs TKE imbalance for desert. Significance: 0.05 level.

Thus it can be stated that the effects of secondary circulations are transported from over the desert towards the forest following the background wind direction, and not the other way around. It is worth noting here that the term ‘secondary circulation’ has been used somewhat loosely here and contain the effects of horizontal transport as well, since partitioning the imbalance term is not possible within the scope of this campaign. In the case of transport from the forest towards the desert, it is more likely that horizontal advection is the main mechanism.

3.4 Effect of nonlocal motions

Figure 6 shows the time series of the triple moments $\overline{w'w'u'}$, $\overline{w'w'w'}$ and $\overline{w'w'T'}$ in the first three rows. The vertical velocity skewness term $\overline{w'w'w'}$ (2nd row) is of importance as it appears in the transport term of the TKE budget (equation 2) and is a measure of non-Gaussian turbulence, which indicates the presence of non-local coherent motions such as sweeps and ejections. Note that the vertical velocity skewness is often negative above the canopy which is consistent with the generic feature of canopy turbulence (Kaimal and Finnigan, 1994; Chamecki, 2013; Dias-Junior et al., 2015). What is perhaps more interesting is that the daytime vertical velocity skewness over the desert is often positive, indicating again of the presence of nonlocal coherent structures active over the desert. The measure of skewness increases over ~~both the forest and the desert~~

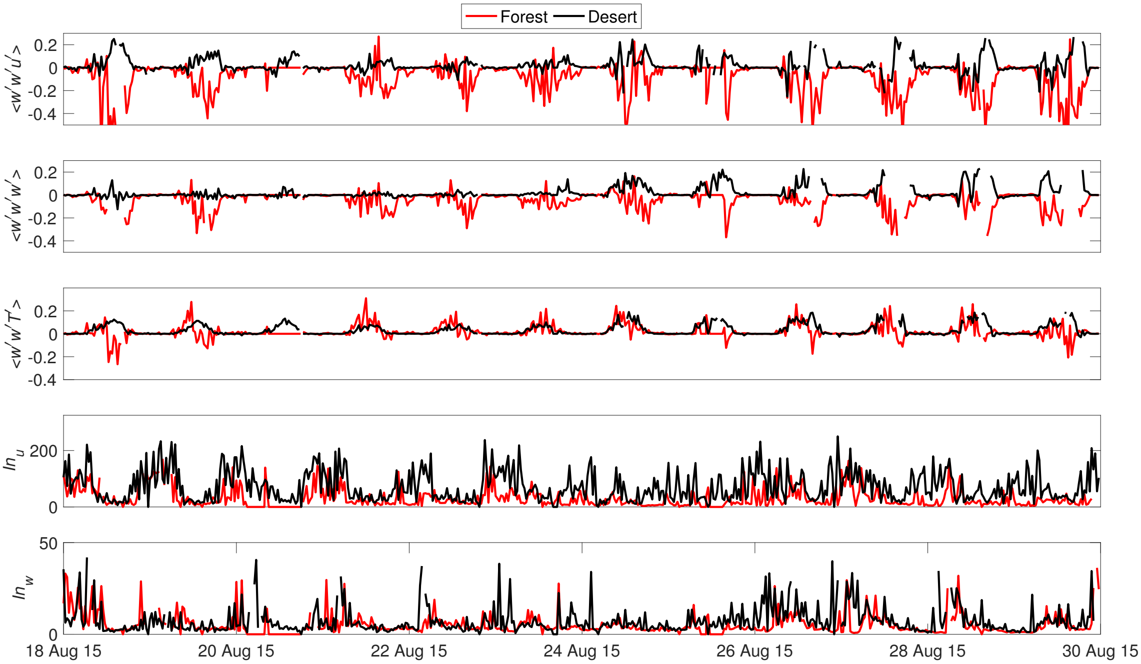

Figure 6. Top three panels: time series of triple moments $\overline{w'w'u'}$, $\overline{w'w'w'}$ (m^3s^{-3}) and $\overline{w'w'T'}$ (~~m^3s^{-3}~~Km^2s^{-2}). Bottom two panels show the integral time scales of horizontal (In_u) and vertical velocities (In_w) in seconds.

~~after 24th August, indicating the arrival of the large scale mesoscale system~~the desert after 23th August. The other two terms $\overline{w'w'u'}$ and $\overline{w'w'T'}$ are also associated with turbulent transport of momentum and heat by as evident from their respective budget equations (Raupach et al., 1986; Zhuang and Amiro, 1994; Cava et al., 2006; Katul et al., 2013; Banerjee et al., 2017b).

$$\frac{\partial \overline{w'u'}}{\partial t} = 0 = -\overline{w'w'}\frac{\partial \overline{U}}{\partial z} - \frac{\partial \left(\overline{w'w'u'}\right)}{\partial z} + \frac{g}{\overline{T}}\overline{u'T'} - \frac{1}{\rho}\left(\overline{u'\frac{\partial p'}{\partial z}}\right); \quad (7)$$

and

$$\frac{\partial \overline{w'T'}}{\partial t} = 0 = -\overline{w'w'}\frac{\partial \overline{T}}{\partial z} - \frac{\partial \left(\overline{w'w'T'}\right)}{\partial z} + \frac{g}{\overline{T}}\overline{T'T'} - \frac{1}{\rho}\left(\overline{T'\frac{\partial p'}{\partial z}}\right). \quad (8)$$

~~Top panel: Boundary layer heights (δ in m) measured using the Doppler LiDARs. Bottom panel: bulk measure of very large scale motion above the forest.~~

Moreover, the triple moments have been shown to be directly correlated with the relative contributions of nonlocal events such as sweeps and ejections as (Nakagawa and Nezu, 1977; Raupach et al., 1986; Cava et al., 2006; Katul et al., 2013; Banerjee et al., 2017b). Notice that momentum transport term $\overline{w'w'u'}$ is also opposite in ~~nature~~ sign for the desert and forest and it shows a strong diurnal cycle. ~~The mesoscale structure after 24th Augustincreases this momentum transport for both the~~

~~forest and~~ After 23th August, increase in momentum transport is noticed for the desert. However, the diurnal cycle of the heat transport term $\overline{w'w'T'}$ is not as strong as its momentum counterpart, but it is often found to be larger over the desert compared to the forest, consistent with the findings from the TKE budget that shows heat is transported from over the desert towards the forest. The fourth and fifth rows of figure 6 show the timeseries of integral timescale of horizontal (In_u) and vertical (In_w) velocity components in seconds. In_u and In_w for every half hour time period are computed by integrating the ~~the~~ normalized autocorrelation function of u and w until the first zero crossing (Kaimal and Finnigan, 1994). They can be interpreted as the characteristic time scale of the most energetic eddies in each direction. As noticed in figure 6, time scales in the horizontal directions are larger compared to the vertical direction. More interesting is the observation that the integral time scales for the eddies above the desert are larger than the forest- ~~both of which increase after 24th. However, this~~ which also increase after 23th. This is another indicator of ~~the transport by secondary circulations above the desert.~~ buoyant production of turbulence, which generates larger eddies than shear production.

3.5 ~~Effect of very large scale motions (VLSM)~~

~~Finally, the effects of the mesoscale structure are further analyzed in figure **??**. The top panel shows the boundary layer heights (δ) over the desert and forest estimated from the backscatter profiles of the Doppler LiDARs. The difference of δ between the desert and forest are not very large although the δ over forest is generally higher than the desert because of the higher levels of turbulenceabove it. δ increases over both the forest and desert after 24th August when Israel is affected by wave activity in the westerlies. We seek to quantify the signature of such a mesoscale system on the turbulence above the desert-forest system and a novel technique is used. Banerjee and Katul (2013a) developed a theoretical framework based on spectral theory to describe the scaling law of the longitudinal velocity variance σ_u^2/u_*^2 in the surface layer. This scaling law includes a bulk parameter α that represents the bulk effects of very large scale motions (VLSM) as well as the boundary layer height δ:~~

$$\cancel{\frac{\sigma_u^2}{u_*^2} = B_1 - A_1 ln\left(\frac{z}{\delta}\right),}$$

~~where~~

$$\cancel{B_1 = C'_{TKE}(1 + ln(\alpha)) + \frac{3}{2}\frac{C''_K}{\kappa^{2/3}}}$$

~~and~~

$$\cancel{A_1 = C'_{TKE};}$$

~~where $C''_K = 0.55$, $\kappa = 0.4$ (von Kármán constant) and $C'_{TKE} = 1.0$. A value of $\alpha > 1$ indicates the presence of VLSM since $ln(1) = 0$. α is computed using equations **??**, **??** and **??** with the experimental data over the forest and plotted in the second panel of figure **??**. The data over the desert is found to be ill conditioned to compute α, however since the synoptic conditions over both the desert and forest are similar as observed from the boundary layer heights, it can be taken as representative for both. As observed, there are a number of large peaks of $\alpha > 1$ after 24th August which confirms the presence of VLSM and~~

~~supports the interpretations of previous findings in this manuscript. It is worth mentioning here that the exact nature/type of the very large scale structures can not be discerned here - i.e., it cannot be pinpointed at a sea-breeze or other mesoscale events. However, a higher value of α would indicate a stronger large scale motion, the effect of which is to include more large scale low frequency motions in the turbulent spectra (Banerjee and Katul, 2013a).~~

4 Conclusions

We studied the nature of turbulent transport over a well defined surface heterogeneity comprising of a desert and forest in the Yatir semi-arid area in Israel. Eddy covariance and Doppler LiDAR measurements were conducted for 12 days between 18th and 31st August, 2015 over two locations in the forest and the shrubland (referred to as 'desert' for the almost complete lack of vegetation during the observation period). Earlier campaigns in this area focused on energy balance closure and hypothesized about the existence of secondary circulations because of surface heterogeneity. The present work was aimed to study the nature of turbulent transport over the forest and the desert in more detail to address the following questions:

1. How does the Yatir forest affect the boundary layer dynamics such as eddy size distribution, boundary layer height and diurnal variations of turbulent statistics and fluxes compared to the surrounding desert?

2. Can the existence of secondary circulation be confirmed?

3. Is there any horizontal energy transport between the forest and the desert and how does it vary with time? ~~What is the effect of mesoscale motions on the turbulent dynamics?~~

To answer the above mentioned questions, we computed half hour average turbulent statistics for both the desert and forest and looked at their diurnal variations. We also computed individual components of the turbulent kinetic energy (TKE) budget and argued that the turbulent transport of energy should be contained in the imbalance of the TKE budget, which consists of the effects of advection, transport by turbulent flux divergence and pressure velocity interactions, since we could not compute those terms explicitly. Moreover, we also computed triple moments which are associated with nonlocal motions and coherent structures and integral time scales, which are associated with the most energetic eddies. We used the measured boundary layer heights to compute a first order bulk parameter which can directly quantify the presence of very large scale motions. The findings to the questions are listed below:

1. The forest is found to be associated with a higher level of turbulent intensity because of higher roughness although the desert reported higher mean speeds and vertical updrafts possibly due to the presence of secondary circulations. Gentle topography around the desert might contribute to the updrafts over the desert as well. The smaller roughness of the desert is also responsible for higher wind speeds above the desert. There is little air temperature difference between the desert and the forest, although the mean velocities and temperature have strong diurnal cycles. Momentum and heat flux are also found to be stronger above the forest. The presence of ~~a large scale system after 24th August seem to strengthen~~ the secondary circulation ~~above the desert and enhance the~~ enhances the turbulent fluxes as well as the turbulent intensity above the desert.

2. The role of secondary circulations can be better understood once the components of the TKE budget are studied. Over the forest the production of turbulence is mechanical, while over the desert, TKE production is mostly carried by buoyancy. The forest is more efficient in dissipating TKE as well. The imbalance of TKE is taken as the indicator of TKE transport and is found to vary diurnally almost anti synchronously over the desert and forest - confirming the role of a secondary circulation. The TKE budget is closed better over the forest compared to the desert. ~~This imbalance and consequently the secondary circulation also varies differently with atmospheric stability. For the desert, it is higher for more stable conditions, possibly indicating of a secondary circulation driven by advection under a temperature inversion.~~ Turbulent triple moments which are indicators of nonlocal motions and coherent structures also show strong variability over the desert and opposite in signs, also confirming the role of secondary circulations. The integral time scales are found to be higher over the desert compared to the forest. This suggests that the secondary circulations that transport energy are more active over the desert- however, they cannot produce much turbulence over the desert since they only rely on buoyancy driven turbulence as mechanical forcing is missing over the desert. This is also highlighted by the fact that mean velocities are higher above the desert while turbulent fluctuations are higher above the forest.

3. To elucidate the role of horizontal transport between the desert and the forest, we studied the correlation between the TKE imbalance over the desert and the TKE production over the forest. The moderately high correlation suggests that the secondary circulation is transported from over the desert towards the forest, enhancing TKE production over the forest. The low correlation between the TKE imbalance over the forest and TKE production over the desert confirms the directionality of this horizontal exchange, which is from the desert towards the forest and not the other way around.

   ~~Weather data confirms that Rossby wave activities in the westerlies influenced the troposphere above Israel after 24th August and reduced the very stable stratification. As a response, the boundary layer heights increased both over the desert and forest. We quantified the first order effect of the very large scale motions (VLSM) through a scaling law that involves the longitudinal turbulent velocity variance developed by Banerjee and Katul (2013a) and found that there are several peaks of a parameter~~ $\cancel{\alpha}$ ~~that contains the bulk effect of all kinds of VLSMs. The VLSMs are found to enhance turbulence fluxes and the nonlocal motions for both the forest and the desert. Although its main effect is to enhance the secondary circulations already existing over the desert transporting energy towards the forest.~~

To summarize, we have examined the existence and role of secondary circulations that exists because of large scale surface heterogeneities and possible due to some topography effects between the desert and forest by looking at proxy quantities computed from turbulence measurements. Although the campaign was conducted at a particular site, the conclusions drawn are fairly general and can be extended to other scenarios involving surface heterogeneities such as urban landscapes, agricultural fields etc. Future works will attempt to highlight a more spatially detailed picture of the turbulent structure under the interesting scenario of secondary circulations and horizontal energy transport.

Acknowledgements. This research was supported by the German Research Foundation (DFG) as part of the project “Climate feedbacks and benefits of semi-arid forests (CliFF)" and the project “Capturing all relevant scales of biosphere-atmosphere exchange - the enigmatic energy balance closure problem”, which is funded by the Helmholtz-Association through the President’s Initiative and Networking Fund, and by KIT. We suggest contacting the principal investigator Dr. Matthias Mauder (matthias.mauder@kit.edu) if one is interested in obtaining the data used in the paper.

Appendix A: Full form of the TKE budget

$$
\begin{aligned}
&\frac{\partial e}{\partial t} + U\frac{\partial e}{\partial x} + V\frac{\partial e}{\partial y} + W\frac{\partial e}{\partial z} = \frac{g}{T}\left(\overline{w'T'}\right)\\
&-\overline{u'u'}\frac{\partial U}{\partial x} - \overline{v'u'}\frac{\partial V}{\partial x} - \overline{w'u'}\frac{\partial W}{\partial x}\\
&-\overline{u'v'}\frac{\partial U}{\partial y} - \overline{v'v'}\frac{\partial V}{\partial y} - \overline{w'v'}\frac{\partial W}{\partial y}\\
&-\overline{u'w'}\frac{\partial U}{\partial z} - \overline{v'w'}\frac{\partial V}{\partial z} - \overline{w'w'}\frac{\partial W}{\partial z}\\
&\qquad -\frac{\partial\left(\overline{u'e}\right)}{\partial x} - \frac{\partial\left(\overline{v'e}\right)}{\partial y} - \frac{\partial\left(\overline{w'e}\right)}{\partial z} - \frac{1}{\rho}\frac{\partial\left(\overline{u'p'}\right)}{\partial x} - \frac{1}{\rho}\frac{\partial\left(\overline{v'p'}\right)}{\partial y} - \frac{1}{\rho}\frac{\partial\left(\overline{w'p'}\right)}{\partial z} - \epsilon,
\end{aligned}
\tag{A1}
$$

Thus to be consistent with equation 2, all the terms in equation A1 that cannot be evaluated using one point measurements can be clubbed in the imbalance term, which can be described by

$$
\begin{aligned}
&Imbalance = \frac{\partial e}{\partial t} + U\frac{\partial e}{\partial x} + V\frac{\partial e}{\partial y} + W\frac{\partial e}{\partial z}\\
&+\overline{u'u'}\frac{\partial U}{\partial x} + \overline{v'u'}\frac{\partial V}{\partial x} + \overline{w'u'}\frac{\partial W}{\partial x}\\
&+\overline{u'v'}\frac{\partial U}{\partial y} + \overline{v'v'}\frac{\partial V}{\partial y} + \overline{w'v'}\frac{\partial W}{\partial y}\\
&+\overline{v'w'}\frac{\partial V}{\partial z} + \overline{w'w'}\frac{\partial W}{\partial z}\\
&\qquad +\frac{\partial\left(\overline{u'e}\right)}{\partial x} + \frac{\partial\left(\overline{v'e}\right)}{\partial y} + \frac{\partial\left(\overline{w'e}\right)}{\partial z} + \frac{1}{\rho}\frac{\partial\left(\overline{u'p'}\right)}{\partial x} + \frac{1}{\rho}\frac{\partial\left(\overline{v'p'}\right)}{\partial y} + \frac{1}{\rho}\frac{\partial\left(\overline{w'p'}\right)}{\partial z}.
\end{aligned}
\tag{A2}
$$

Thus if no assumptions or idealizations are invoked, the imbalance of the commonly used operational TKE budget (equation 2) consists of TKE tendency, advection, shear production, TKE flux divergence and pressure velocity interactions. Using an array of sonics in each direction will enable determination of all these terms. However, as evident from the myriad of terms contributing to the imbalance, it is difficult to determine what degree of assumptions of homogeneity in which direction are sufficient so that certain terms can be ignored. Thus unless all terms in equation A2 can be determined, it is easier to stick to the most idealized form of equation 2 and treat all other terms as imbalances. Future work will try to determine the partitioning of advection, flux divergence and the other shear production terms contributing to TKE budget imbalances in presence of heterogeneities.

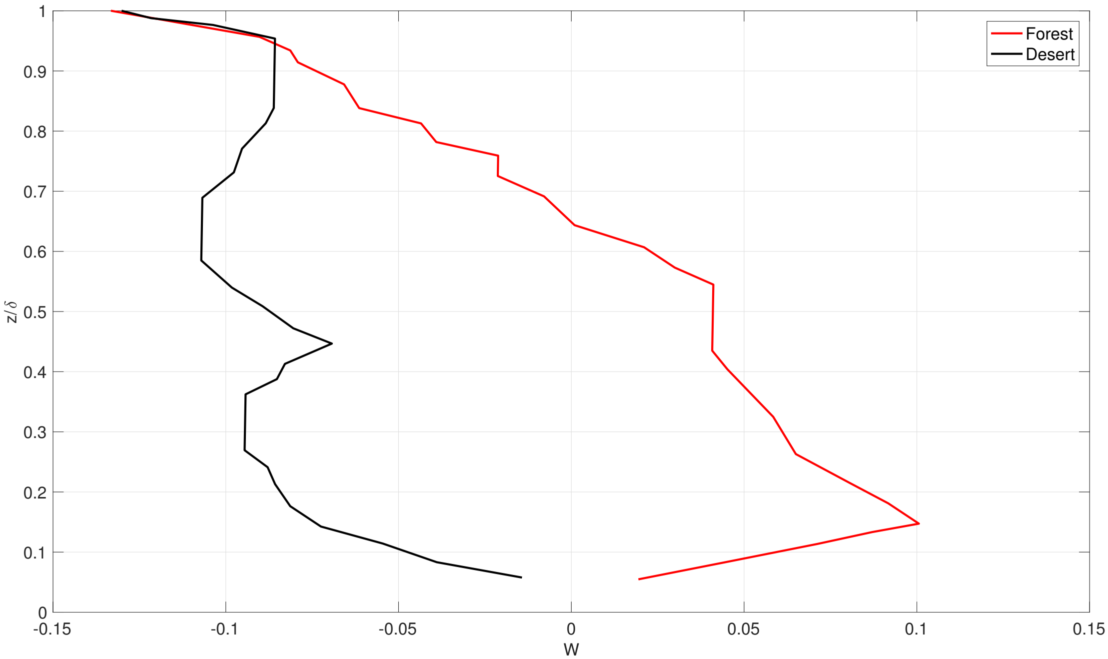

Figure 7. Mean vertical velocity ms^{-1} above the forest and the desert as measured by LiDARs.

Appendix B: Further evidence of secondary circulation

Figure shows mean vertical velocity W above the forest and the desert averaged over all observations using the Doppler LiDARS. Note that there is a mean updraft ($W > 0$) above the forest and a mean downdraft above the desert ($W < 0$). This suggests that there exists a mean secondary circulation and supports the findings and observations in the manuscript.

Appendix C: Details of coordinate rotation of turbulence velocity measurements

A planar fit method described by Wilczak et al. (2001) is used, which considers the tilt of the sonic anemometer with respect to local streamlines. Hence this technique is deemed to be more suitable in the presence of sloped terrain, which can be associated with a net non-zero mean vertical velocity. The hypothesis being employed is that under the condition of tilting relative to the local streamlines, a portion of the horizontal velocities will be present in the measured vertical velocity component:

$$\overline{w}_m = b_1 \overline{u}_m + b_2 \overline{v}_m, \tag{C1}$$

where over-bars denote half hour time averaging and the subscript m indicates measured velocity components. Note that this is a modification of the original Wilczak et al. (2001) formulation by Van Dijk et al. (2004), who noted that the equation C1 does not need an additional constant. b_1 and b_2 are computed using a bilinear regression using all the data points for individual sonic anemometers. Next, to orient the z axis perpendicular to the local streamlines, a rotation is performed:

$$[u_{pf};v_{pf};w_{pf}]=[M_{pf}][u_m;v_m;w_m] \tag{C2}$$

where the rotation matrix is defined as

$$M_{pf}=\begin{bmatrix} cos\alpha & 0 & -sin\alpha \\ 0 & 1 & 0 \\ sin\alpha & 0 & cos\alpha \end{bmatrix}\begin{bmatrix} 1 & 0 & 0 \\ 0 & cos\beta & sin\beta \\ 0 & -sin\beta & cos\beta \end{bmatrix},$$

where $tan\,\alpha=-b_1$ and $tan\,\beta=b_2$ (from which $sin\,\alpha$, $cos\,\alpha$, $sin\,\beta$ and $cos\,\beta$ can be computed). Finally, another rotation is applied to align the wind vector with the mean wind direction:

$$u_{rot}=u_{pf}\,cos\,\theta+v_{pf}\,sin\,\theta; v_{rot}=-u_{pf}\,sin\,\theta+v_{pf}\,cos\,\theta; v_{rot}=w_{pf}, \tag{C3}$$

where $\theta=tan^{-1}(v_{pf}/u_{pf})$. This also ensures that the crosswind (v) component is zero.

References

Banerjee, T. and Katul, G.: Logarithmic scaling in the longitudinal velocity variance explained by a spectral budget, Physics of Fluids (1994-present), 25, 125 106, 2013a.

Banerjee, T., Katul, G., Fontan, S., Poggi, D., and Kumar, M.: Mean flow near edges and within cavities situated inside dense canopies, Boundary-Layer Meteorology, 149, 19–41, 2013.

Banerjee, T., Katul, G., Salesky, S., and Chamecki, M.: Revisiting the formulations for the longitudinal velocity variance in the unstable atmospheric surface layer, Quarterly Journal of the Royal Meteorological Society, 141, 1699–1711, 2015.

Banerjee, T., Li, D., Juang, J.-Y., and Katul, G.: A spectral budget model for the longitudinal turbulent velocity in the stable atmospheric surface layer, Journal of the Atmospheric Sciences, 73, 145–166, 2016.

Banerjee, T., De Roo, F., and Mauder, M.: Explaining the convector effect in canopy turbulence by means of large-eddy simulation, Hydrology and Earth System Sciences, 21, 2987, 2017a.

Banerjee, T., De Roo, F., and Mauder, M.: Connecting the Failure of K Theory inside and above Vegetation Canopies and Ejection–Sweep Cycles by a Large-Eddy Simulation, Journal of Applied Meteorology and Climatology, 56, 3119–3131, 2017b.

Belcher, S. E., Jerram, N., and Hunt, J. C. R.: Adjustment of a Turbulent Boundary Layer to a Canopy of Roughness Elements, Journal of Fluid Mechanics, 488, 369–398, 2003.

Businger, J. A., Wyngaard, J. C., Izumi, Y., and Bradley, E. F.: Flux-profile relationships in the atmospheric surface layer, Journal of the Atmospheric Sciences, 28, 181–189, 1971.

Cassiani, M., Katul, G. G., and Albertson, J. D.: The Effects of Canopy Leaf Area Index on Airflow across Foest Edges: Large-Eddy Simulation and Analytical Results, Boundary-Layer Meteorology, 126, 433–460, 2008.

Cava, D., Katul, G., Scrimieri, A., Poggi, D., Cescatti, A., and Giostra, U.: Buoyancy and the sensible heat flux budget within dense canopies, Boundary-Layer Meteorology, 118, 217–240, 2006.

Chamecki, M.: Persistence of velocity fluctuations in non-Gaussian turbulence within and above plant canopies, Physics of Fluids (1994-present), 25, 115 110, 2013.

Chatziefstratiou, E. K., Velissariou, V., and Bohrer, G.: Resolving the effects of aperture and volume restriction of the flow by semi-porous barriers using large-eddy simulations, Boundary-layer meteorology, 152, 329–348, 2014.

Courault, D., Drobinski, P., Brunet, Y., Lacarrere, P., and Talbot, C.: Impact of surface heterogeneity on a buoyancy-driven convective boundary layer in light winds, Boundary-Layer Meteorology, 124, 383–403, 2007.

Dalpe, B. and Masson, C.: Numerical Simulation of Wind Flow near a Forest Edge, Journal of Wind Engineering and Industrial Aerodynamics, 97, 228–241, 2009.

Dalu, G. and Pielke, R.: Vertical heat fluxes generated by mesoscale atmospheric flow induced by thermal inhomogeneities in the PBL, Journal of the Atmospheric Sciences, 50, 919–926, 1993.

Detto, M., Katul, G. G., Siqueira, M., Juang, J. Y., and Stoy, P.: The Structure of Turbulence near a Tall Forest Edge: The Backward-Facing Step Flow Analogy Revisited, Ecological Applications, 18, 1420–1435, 2008.

Dias-Junior, C. Q., Marques Filho, E. P., and Sá, L. D.: A large eddy simulation model applied to analyze the turbulent flow above Amazon forest, Journal of Wind Engineering and Industrial Aerodynamics, 147, 143–153, 2015.

Dixon, N., Parker, D., Taylor, C., Garcia-Carreras, L., Harris, P., Marsham, J., Polcher, J., and Woolley, A.: The effect of background wind on mesoscale circulations above variable soil moisture in the Sahel, Quarterly Journal of the Royal Meteorological Society, 139, 1009–1024, 2013.

Dupont, S. and Brunet, Y.: Coherent structures in canopy edge flow: a large-eddy simulation study, Journal of Fluid Mechanics, 630, 93–128, 2009.

Dyer, A.: A review of flux-profile relationships, Boundary-Layer Meteorology, 7, 363–372, 1974.

Eder, F., De Roo, F., Kohnert, K., Desjardins, R. L., Schmid, H. P., and Mauder, M.: Evaluation of two energy balance closure parametrizations, Boundary-Layer Meteorology, 151, 195–219, 2014.

Eder, F., De Roo, F., Rotenberg, E., Yakir, D., Schmid, H. P., and Mauder, M.: Secondary circulations at a solitary forest surrounded by semi-arid shrubland and their impact on eddy-covariance measurements, Agricultural and Forest Meteorology, 211, 115–127, 2015.

Fesquet, C., Dupont, S., Drobinski, P., Dubos, T., and Barthlott, C.: Impact of Terrain Heterogeneity on Coherent Structure Properties: Numerical Approach, Boundary-Layer Meteorology, 133, 71–92, 2009.

Foken, T.: The energy balance closure problem: an overview, Ecological Applications, 18, 1351–1367, 2008.

Fuentes, J. D., Chamecki, M., Nascimento dos Santos, R. M., Von Randow, C., Stoy, P. C., Katul, G., Fitzjarrald, D., Manzi, A., Gerken, T., Trowbridge, A., et al.: Linking meteorology, turbulence, and air chemistry in the Amazon rainforest, Bulletin of the American Meteorological Society, 2016.

Garcia-Carreras, L., Parker, D. J., Taylor, C. M., Reeves, C. E., and Murphy, J. G.: Impact of mesoscale vegetation heterogeneities on the dynamical and thermodynamic properties of the planetary boundary layer, Journal of Geophysical Research: Atmospheres, 115, 2010.

Gavrilov, K., Accary, G., Morvan, D., Lyubimov, D., Bessonov, O., and Meradji, S.: Large Eddy Simulation of Coherent Structures over Forest Canopy, Turbulence and Interactions, 110, 143–149, 2010.

Gavrilov, K., Accary, G., Morvan, D., Lyubimov, D., Meradji, S., and Bessonov, O.: Numerical Simulation of Coherent Structures over Plant Canopy, Flow Turbulence and Combustion, 86, 89–111, 2011.

Harman, I. N. and Finnigan, J. J.: A simple unified theory for flow in the canopy and roughness sublayer, Boundary-layer meteorology, 123, 339–363, 2007.

Higgins, C. W., Katul, G. G., Froidevaux, M., Simeonov, V., and Parlange, M. B.: Are atmospheric surface layer flows ergodic?, Geophysical Research Letters, 40, 3342–3346, 2013.

Huang, J., Cassiani, M., and Albertson, J. D.: Coherent Turbulent Structures across a Vegetation Discontinuity, Boundary-Layer Meteorology, 140, 1–22, 2011.

Irvine, M. R., Gardiner, B. A., and Hill, M. K.: The Evolution of Turbulence across a Forest Edge, Boundary-Layer Meteorology, 84, 467–496, 1997.

Kaimal, J. C. and Finnigan, J. J.: Atmospheric boundary layer flows: their structure and measurement, Oxford University Press, 1994.

Kanani-Sühring, F. and Raasch, S.: Spatial variability of scalar concentrations and fluxes downstream of a clearing-to-forest transition: a large-eddy simulation study, Boundary-Layer Meteorology, 155, 1–27, 2015.

Kanda, M., Inagaki, A., Letzel, M. O., Raasch, S., and Watanabe, T.: LES study of the energy imbalance problem with eddy covariance fluxes, Boundary-Layer Meteorology, 110, 381–404, 2004.

Kang, S.-L. and Lenschow, D. H.: Temporal evolution of low-level winds induced by two-dimensional mesoscale surface heat-flux heterogeneity, Boundary-Layer Meteorology, 151, 501–529, 2014.

Katul, G. G., Cava, D., Siqueira, M., and Poggi, D.: Scalar turbulence within the canopy sublayer, Coherent Flow Structures at Earth's Surface, pp. 73–95, 2013.

Kröniger, K., Banerjee, T., De Roo, F., and Mauder, M.: Flow adjustment inside homogeneous canopies after a leading edge–An analytical approach backed by LES, Agricultural and Forest Meteorology, 2017.

Li, D., Salesky, S. T., and Banerjee, T.: Connections between the Ozmidov scale and mean velocity profile in stably stratified atmospheric surface layers, Journal of Fluid Mechanics, 797, R3, 2016.

Li, Z. J., Lin, J. D., and Miller, D. R.: Air-Flow over and through a Forest Edge - a Steady-State Numerical-Simulation, Boundary-Layer Meteorology, 51, 179–197, 1990.

Lotteraner, C. and Piringer, M.: Mixing-Height Time Series from Operational Ceilometer Aerosol-Layer Heights, Boundary-Layer Meteorology, 161, 265–287, 2016.

Mahfouf, J.-F., Richard, E., and Mascart, P.: The influence of soil and vegetation on the development of mesoscale circulations, Journal of Applied Meteorology and Climatology, 26, 1483–1495, 1987.

Markfort, C., Porté-Agel, F., and Stefan, H.: Canopy-wake dynamics and wind sheltering effects on Earth surface fluxes, Environmental Fluid Mechanics, 14, 663–697, 2014.

Marusic, I., Monty, J. P., Hultmark, M., and Smits, A. J.: On the logarithmic region in wall turbulence, Journal of Fluid Mechanics, 716, R3, 2013.

Mauder, M., Jegede, O., Okogbue, E., Wimmer, F., and Foken, T.: Surface energy balance measurements at a tropical site in West Africa during the transition from dry to wet season, Theoretical and Applied Climatology, 89, 171–183, 2007.

Monin, A. and Obukhov, A.: Basic laws of turbulent mixing in the surface layer of the atmosphere, Contrib. Geophys. Inst. Acad. Sci. USSR, 151, e187, 1954.

Nadeau, D. F., Pardyjak, E. R., Higgins, C. W., Fernando, H. J. S., and Parlange, M. B.: A simple model for the afternoon and early evening decay of convective turbulence over different land surfaces, Boundary-layer meteorology, 141, 301, 2011.

Nakagawa, H. and Nezu, I.: Prediction of the contributions to the Reynolds stress from bursting events in open-channel flows, Journal of Fluid Mechanics, 80, 99–128, 1977.

Peltola, H.: Model Computations on Wind Flow and Turning Moment for Scots Pines along the Margins of Clear-Cut Areas, Forest Ecology and Management, 83, 203–215, 1996.

Perry, A. and Chong, M.: On the mechanism of wall turbulence, Journal of Fluid Mechanics, 119, 173–217, 1982.

Queck, R., Bernhofer, C., Bienert, A., and Schlegel, F.: The TurbEFA Field Experiment - Measuring the Influence of a Forest Clearing on the Turbulent Wind Field, Boundary-Layer Meteorology, pp. 1–27, 2016.

Raupach, M. and Finnigan, J.: Scale issues in boundary-layer meteorology: Surface energy balances in heterogeneous terrain, Hydrological Processes, 9, 589–612, 1995.

Raupach, M., Coppin, P., and Legg, B.: Experiments on scalar dispersion within a model plant canopy part I: The turbulence structure, Boundary-Layer Meteorology, 35, 21–52, 1986.

Rominger, J. T. and Nepf, H. M.: Flow Adjustment and Interior Flow Associated with a Rectangular Porous Obstruction, Journal of Fluid Mechanics, 680, 636–659, 2011.

Rotenberg, E. and Yakir, D.: Distinct patterns of changes in surface energy budget associated with forestation in the semiarid region, Global change biology, 17, 1536–1548, 2011.

Salesky, S. T., Katul, G. G., and Chamecki, M.: Buoyancy effects on the integral lengthscales and mean velocity profile in atmospheric surface layer flows, Physics of Fluids (1994-present), 25, 105 101, 2013.

Schlegel, F., Stiller, J., Bienert, A., Maas, H. G., Queck, R., and Bernhofer, C.: Large-Eddy Simulation of Inhomogeneous Canopy Flows Using High Resolution Terrestrial Laser Scanning Data, Boundary-Layer Meteorology, 142, 223–243, 2012.

Stoy, P. C., Mauder, M., Foken, T., Marcolla, B., Boegh, E., Ibrom, A., Arain, M. A., Arneth, A., Aurela, M., Bernhofer, C., et al.: A data-driven analysis of energy balance closure across FLUXNET research sites: The role of landscape scale heterogeneity, Agricultural and forest meteorology, 171, 137–152, 2013.

Stull, R. B.: An introduction to boundary layer meteorology, vol. 13, Springer Science & Business Media, 2012.

Sühring, M. and Raasch, S.: Heterogeneity-induced heat-flux patterns in the convective boundary layer: can they be detected from observations and is there a blending height? - a large-eddy simulation study for the LITFASS-2003 experiment, Boundary-Layer Meteorology, 148, 309–331, 2013.

Townsend, A. A.: The structure of turbulent shear flow, Cambridge university press, 1976.

Van Dijk, A., Moene, A., De Bruin, H., et al.: The principles of surface flux physics: theory, practice and description of the ECPACK library, Internal Rep, 1, 99, 2004.

van Heerwaarden, C. C. and Guerau de Arellano, J. V.: Relative humidity as an indicator for cloud formation over heterogeneous land surfaces, Journal of the Atmospheric Sciences, 65, 3263–3277, 2008.

Van Heerwaarden, C. C., Mellado, J. P., and De Lozar, A.: Scaling laws for the heterogeneously heated free convective boundary layer, Journal of the Atmospheric Sciences, 71, 3975–4000, 2014.

Wilczak, J. M., Oncley, S. P., and Stage, S. A.: Sonic anemometer tilt correction algorithms, Boundary-Layer Meteorology, 99, 127–150, 2001.

Yang, B., Raupach, M. R., Shaw, R. H., Tha, K., Paw, U., and Morse, A. P.: Large-Eddy Simulation of Turbulent Flow across a Forest Edge. Part I: Flow Statistics, Boundary-Layer Meteorology, 120, 377–412, 2006.

Yue, P., Zhang, Q., Wang, R., Li, Y., and Wang, S.: Turbulence intensity and turbulent kinetic energy parameters over a heterogeneous terrain of Loess Plateau, Advances in Atmospheric Sciences, 32, 1291–1302, 2015.

Zhuang, Y. and Amiro, B.: Pressure fluctuations during coherent motions and their effects on the budgets of turbulent kinetic energy and momentum flux within a forest canopy, Journal of Applied Meteorology, 33, 704–711, 1994.